# DNA-binding affinity and specificity determine the phenotypic diversity in *BCL11B*-related disorders

## Graphical abstract
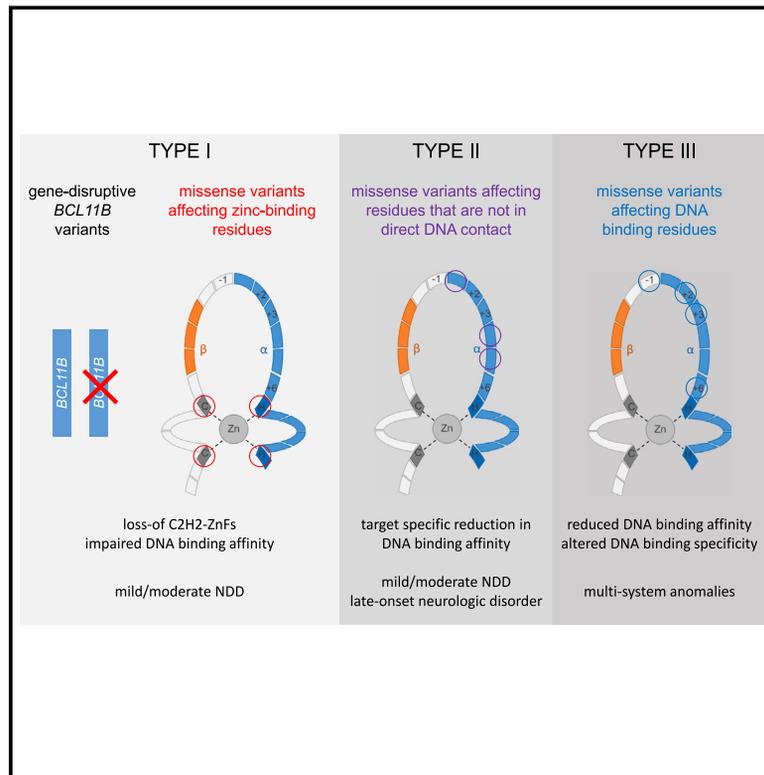


## Authors

Ivana Lessel, Anja Baresic,
Ivan K. Chinn, ..., James R. Lupski,
Eva Tolosa, Davor Lessel

## Correspondence

davor.lessel@klinik.uni-regensburg.de

**Combining genotype-phenotype data of 92 individuals harboring a pathogenic *BCL11B* variant, with immune phenotyping, analysis of chromatin immunoprecipitation DNA-sequencing data, dual-luciferase reporter assays, and molecular modeling, the authors show here that nearby missense variants and different missense variants affecting the identical amino acid do not necessarily cause similar clinical outcomes.**

CellPress

# ARTICLE

# DNA-binding affinity and specificity determine the phenotypic diversity in *BCL11B*-related disorders

Ivana Lessel,[1,2,86] Anja Baresic,[3,86] Ivan K. Chinn,[4,5] Jonathan May,[6] Anu Goenka,[7,8]
Kate E. Chandler,[7,8] Jennifer E. Posey,[9] Alexandra Afenjar,[10] Luisa Averdunk,[11,12]
Maria Francesca Bedeschi,[13] Thomas Besnard,[14,15] Rae Brager,[16] Lauren Brick,[17] Melanie Brugger,[18,19]
Theresa Brunet,[18] Susan Byrne,[20] Oscar de la Calle-Martín,[21] Valeria Capra,[22] Paul Cardenas,[23]
Céline Chappé,[24] Hey J. Chong,[25] Benjamin Cogne,[14,15] Erin Conboy,[26] Heidi Cope,[27]
Thomas Courtin,[28] Wallid Deb,[14,15] Robertino Dilena,[29] Christèle Dubourg,[30,31] Magdeldin Elgizouli,[32]
Erica Fernandes,[33] Kristi K. Fitzgerald,[34] Silvana Gangi,[35] Jaya K. George-Abraham,[36,37]
Muge Gucsavas-Calikoglu,[38] Tobias B. Haack,[39] Medard Hadonou,[40] Britta Hanker,[41] Irina Hüning,[41]
Maria Iascone,[42] Bertrand Isidor,[14,15] Irma Järvelä,[43] Jay J. Jin,[44]

*(Author list continued on next page)*

## Summary

BCL11B is a Cys2-His2 zinc-finger (C2H2-ZnF) domain-containing, DNA-binding, transcription factor with established roles in the development of various organs and tissues, primarily the immune and nervous systems. *BCL11B* germline variants have been associated with a variety of developmental syndromes. However, genotype-phenotype correlations along with pathophysiologic mechanisms of selected variants mostly remain elusive. To dissect these, we performed genotype-phenotype correlations of 92 affected individuals harboring a pathogenic or likely pathogenic *BCL11B* variant, followed by immune phenotyping, analysis of chromatin immunoprecipitation DNA-sequencing data, dual-luciferase reporter assays, and molecular modeling. These integrative analyses enabled us to define three clinical subtypes of *BCL11B*-related disorders. It is likely that gene-disruptive *BCL11B* variants and missense variants affecting zinc-binding cysteine and histidine residues cause mild to moderate neurodevelopmental delay with increased propensity for behavioral and dental anomalies, allergies and asthma, and reduced type 2 innate lymphoid cells. Missense variants within C2H2-ZnF DNA-contacting α helices cause highly variable clinical presentations ranging from multisystem anomalies with demise in the first years of life to late-onset, hyperkinetic movement disorder with poor fine motor skills. Those not in direct DNA contact cause a milder phenotype through reduced, target-specific transcriptional activity. However, missense variants affecting C2H2-ZnFs, DNA binding, and "specificity residues" impair BCL11B transcriptional activity in a target-specific, dominant-negative manner along with aberrant regulation of alternative DNA targets, resulting in more severe and unpredictable clinical outcomes. Taken together, we suggest that the phenotypic severity and variability is largely dependent on the DNA-binding affinity and specificity of altered BCL11B proteins.

## Introduction

Proteins containing a Cys2-His2 zinc-finger domain (C2H2-ZnF) constitute the largest class of human transcription factors.[1] They act by either repressing or activating the expression of target genes through binding a specific DNA sequence by their tandem and modular C2H2-ZnFs. Each C2H2-ZnF shares a consensus sequence

[1]Institute of Human Genetics, University Medical Center Hamburg-Eppendorf, 20246 Hamburg, Germany; [2]Institute of Human Genetics, University of Regensburg, 93053 Regensburg, Germany; [3]Division of Computing and Data Science, Ruđer Bošković Institute, 10000 Zagreb, Croatia; [4]Department of Pediatrics, Baylor College of Medicine, Houston, TX 77030, USA; [5]Section of Immunology, Allergy, and Retrovirology, Texas Children's Hospital, Houston, TX 77030, USA; [6]Institute of Immunology, University Medical Center Hamburg-Eppendorf, 20246 Hamburg, Germany; [7]Manchester Centre for Genomic Medicine, St Mary's Hospital, Manchester University NHS Foundation Trust, Health Innovation Manchester, Manchester, UK; [8]Division of Evolution, Infection & Genomic Sciences, School of Biological Sciences, Faculty of Biology, Medicine and Health, University of Manchester, Manchester, UK; [9]Department of Molecular and Human Genetics, Baylor College of Medicine, Houston, TX 77030, USA; [10]Département de Génétique Paris, Centre de Référence Malformations et maladies congénitales du cervelet et déficiences intellectuelles de causes rares, APHP, Sorbonne Université, Paris, France; [11]Institute of Human Genetics, Medical Faculty and University Hospital, Heinrich Heine University, Düsseldorf, Germany; [12]Department of General Pediatrics, Neonatology and Pediatric Cardiology, University Children's Hospital, Heinrich-Heine-University, 40225 Düsseldorf, Germany; [13]Fondazione IRCCS Ca' Granda Ospedale Maggiore Policlinico, Medical Genetics Unit, Milan, Italy; [14]L'Institut du Thorax, INSERM, CNRS, Université de Nantes, 44007 Nantes, France; [15]Service de Génétique Médicale, CHU Nantes, 9 quai Moncousu, 44093 Nantes, France; [16]Division of Rheumatology, Immunology and Allergy, McMaster Children's Hospital, Hamilton, ON L8S 4K1, Canada; [17]Division of Genetics and Metabolics, McMaster Children's Hospital, Hamilton, ON L8S 4K1, Canada; [18]Institute of Human Genetics, Klinikum rechts der Isar, School of Medicine, Technical University of Munich, Munich, Germany; [19]Department of Obstetrics and Gynecology, Klinikum Rechts der Isar, Technical University of Munich, Munich, Germany; [20]Department of Paediatric Neurology, Neuromuscular Service, Evelina's Children Hospital, Guy's & St. Thomas' Hospital NHS Foundation Trust, London, UK; [21]Immunology Department, Hospital de la Santa Creu i Sant Pau, Barcelona, Spain; [22]Genomics and Clinical Genetics Unit, IRCCS Istituto Giannina Gaslini, Genoa, Italy; [23]Nicklaus Children's Hospital, Miami, FL, USA; [24]Service d'oncohematologie pédiatrique, CHU Rennes, 35000 Rennes, France; [25]Department of Pediatrics, University of Pittsburgh School of Medicine, UPMC Children's Hospital, Pittsburgh, PA 15224, USA; [26]Department of Medical and Molecular Genetics, Indiana University School of Medicine, Indianapolis, IN, USA; [27]Division of Medical Genetics, Department of Pediatrics, Duke University Medical Center, Durham, NC, USA; [28]Département de

*(Affiliations continued on next page)*

Alexander A.L. Jorge,[45,46] Dragana Josifova,[47] Ruta Kalinauskiene,[47] Erik-Jan Kamsteeg,[48] Boris Keren,[28] Elena Kessler,[49] Heike Kölbel,[50] Mariya Kozenko,[17] Christian Kubisch,[1] Alma Kuechler,[32] Suzanne M. Leal,[51,52] Juha Leppälä,[53] Sharon M. Luu,[26] Gholson J. Lyon,[54,55,56] Suneeta Madan-Khetarpal,[57] Margherita Mancardi,[58] Elaine Marchi,[54] Lakshmi Mehta,[59] Beatriz Menendez,[60] Chantal F. Morel,[61] Sue Moyer Harasink,[33] Dayna-Lynn Nevay,[61] Vincenzo Nigro,[62,63] Sylvie Odent,[64,65] Renske Oegema,[66] John Pappas,[67] Matthew T. Pastore,[68,69] Yezmin Perilla-Young,[38] Konrad Platzer,[70] Nina Powell-Hamilton,[71] Rachel Rabin,[67] Aisha Rekab,[59] Raissa C. Rezende,[46] Leema Robert,[47] Ferruccio Romano,[22] Marcello Scala,[72,73] Karin Poths,[39] Isabelle Schrauwen,[74] Jessica Sebastian,[57] John Short,[40] Richard Sidlow,[75] Jennifer Sullivan,[27] Katalin Szakszon,[76] Queenie K.G. Tan,[27] Undiagnosed Diseases Network,[77] Matias Wagner,[18,78,79] Dagmar Wieczorek,[11] Bo Yuan,[9,80] Nicole Maeding,[81] Dirk Strunk,[81] Amber Begtrup,[82] Siddharth Banka,[7,8] James R. Lupski,[4,9,80,83] Eva Tolosa,[6,84] and Davor Lessel[1,2,85,*]

that folds in the presence of zinc ($Zn^{2+}$) to form a two-stranded antiparallel β sheet and a DNA-contacting α helix. Indeed, ionic bonds between zinc and the two cysteines and two histidines, within each C2H2-ZnF, provide the structural stability of these domains.[2] Each C2H2-ZnF typically contacts three base pairs,[3] whereas the exact DNA binding and sequence preference is mainly regulated by the four "specificity residues" at amino acid positions −1, +2, +3, and +6 within the α helix.[2,4] In line with their great abundance, C2H2-ZnF-containing proteins are involved in diverse biological processes including development and differentiation of various organs and tissues.[5,6] Pathogenic variants in genes encoding for C2H2-ZnF-containing proteins are associated with a broad variety of human diseases, including more than 70 associated with a neurodevelopmental or a neurologic disorder.[7]

*BCL11B* (RefSeq NM_138576.3, MIM: 606558), a member of the Krüppel-like family encoding for B cell

Génétique, Hôpital La Pitié-Salpêtrière, Assistance Publique-Hôpitaux de Paris, Paris, France; [29]Fondazione IRCCS Ca' Granda Ospedale Maggiore Policlinico, Neuropathophysiology Unit, Milan, Italy; [30]Service de Génétique Moléculaire et Génomique, CHU, 35033 Rennes, France; [31]University Rennes, CNRS, IGDR, UMR 6290, 35000 Rennes, France; [32]Institut für Humangenetik, Universitätsklinikum Essen, Universität Duisburg-Essen, Essen, Germany; [33]Division of Genetics, Department of Pediatrics, Nemours Children's Health, Wilmington, DE, USA; [34]Department of Cardiology, Nemours Children's Hospital, Wilmington, DE, USA; [35]Neonatal Intensive Care Unit, Fondazione IRCCS Ca' Granda Ospedale Maggiore Policlinico, Via Francesco Sforza, 28, 20122 Milan, Italy; [36]Dell Children's Medical Group, Austin, TX, USA; [37]Department of Pediatrics, The University of Texas at Austin Dell Medical School, Austin, TX, USA; [38]Division of Genetics and Metabolism, Department of Pediatrics, University of North Carolina at Chapel Hill School of Medicine, Chapel Hill, NC 27599, USA; [39]Institute of Medical Genetics and Applied Genomics, University of Tübingen, Tübingen, Germany; [40]South West Thames Centre for Genomics, St George's University Hospitals NHS Foundation Trust, London SW17 0QT, UK; [41]Institute of Human Genetics, University of Lübeck, Lübeck, Germany; [42]Medical Genetics Laboratory, ASST Papa Giovanni XXIII, 24128 Bergamo, Italy; [43]Department of Medical Genetics, University of Helsinki, P.O. Box 720, 00251 Helsinki, Finland; [44]Division of Pediatric Pulmonology, Allergy, and Sleep Medicine, Riley Hospital for Children, Indiana University School of Medicine, Indianapolis, IN, USA; [45]Unidade de Endocrinologia do Desenvolvimento, Laboratorio de Hormonios e Genetica Molecular (LIM42), Hospital das Clinicas da Faculdade de Medicina, Universidade de São Paulo (USP), São Paulo, Brazil; [46]Unidade de Endocrinologia Genetica (LIM25), Hospital das Clinicas da Faculdade de Medicina, Universidade de São Paulo (USP), São Paulo, Brazil; [47]Department of Clinical Genetics, Guy's and St. Thomas' NHS Foundation Trust, London, UK; [48]Department of Human Genetics, Radboud University Medical Center, Nijmegen, the Netherlands; [49]Division of Pediatric Hematology/Oncology, Department of Pediatrics, University of Pittsburgh School of Medicine, Pittsburgh, PA, USA; [50]Department of Pediatric Neurology, Centre for Neuromuscular Disorders, Centre for Translational Neuro- and Behavioral Sciences, University Hospital Essen, Essen, Germany; [51]Department of Neurology, Center for Statistical Genetics, Gertrude H. Sergievsky Center, Columbia University Medical Center, Columbia University, New York, NY 10032, USA; [52]Taub Institute for Alzheimer's Disease and the Aging Brain, Columbia University Medical Center, New York, NY, USA; [53]The Wellbeing Services County of South Ostrobothnia, 60280 Seinäjoki, Finland; [54]Department of Human Genetics, New York State Institute for Basic Research in Developmental Disabilities, New York, NY, USA; [55]George A. Jervis Clinic, NYS Institute for Basic Research in Developmental Disabilities, Staten Island, NY, USA; [56]Biology PhD Program, The Graduate Center, The City University of New York, New York, NY, USA; [57]Department of Pediatrics, Division of Medical Genetics and Genomic Medicine, UPMC Children's Hospital of Pittsburgh, Pittsburgh, PA, USA; [58]Unit of Child Neuropsychiatry, IRCCS Istituto Giannina Gaslini, Epicare Network for Rare Disease, Genoa, Italy; [59]Department of Pediatrics, Division of Clinical Genetics, Columbia University Irving Medical Center, New York, NY, USA; [60]Division of Genetics, University of Illinois College of Medicine, Chicago, IL 60612, USA; [61]Fred A. Litwin Family Centre in Genetic Medicine, Department of Medicine, University Health Network, Toronto, ON, Canada; [62]Department of Precision Medicine, University of Campania "Luigi Vanvitelli", Naples, Italy; [63]Telethon Institute of Genetics and Medicine, Pozzuoli, Italy; [64]Clinical Genetics, Centre de Référence Maladies Rares CLAD-Ouest, ERN-ITHACA, FHU GenOMedS, CHU de Rennes, Rennes, France; [65]University Rennes, CNRS, INSERM, Institut de génétique et développement de Rennes, UMR 6290, ERL U1305, Rennes, France; [66]Department of Genetics, University Medical Center Utrecht, Utrecht University, 3584 EA Utrecht, the Netherlands; [67]Department of Pediatrics, New York University Grossman School of Medicine, New York, NY 10016, USA; [68]Division of Genetic and Genomic Medicine, Nationwide Children's Hospital, Columbus, OH, USA; [69]Department of Pediatrics, The Ohio State University College of Medicine, Columbus, OH, USA; [70]Institute of Human Genetics, University of Leipzig Medical Center, 04103 Leipzig, Germany; [71]Division of Medical Genetics, Nemours Children's Hospital, Wilmington, DE, USA; [72]Department of Neurosciences, Rehabilitation, Ophthalmology, Genetics, Maternal and Child Health, University of Genoa, 16145 Genoa, Italy; [73]U.O.C. Genetica Medica, IRCCS Istituto Giannina Gaslini, Genoa, Italy; [74]Department of Translational Neurosciences, University of Arizona College of Medicine – Phoenix, Phoenix, AZ 85004, USA; [75]Department of Medical Genetics and Metabolism, Valley Children's Hospital, Madera, CA, USA; [76]Institute of Pediatrics, Faculty of Medicine, University of Debrecen, 4032 Debrecen, Hungary; [77]Undiagnosed Diseases Network, NIH, Bethesda, MD, USA; [78]Institute of Neurogenomics, Helmholtz Zentrum München, Neuherberg, Germany; [79]Department of Pediatrics, Division of Pediatric Neurology, Developmental Medicine and Social Pediatrics, University Hospital of Munich, Munich, Germany; [80]Human Genome Sequencing Center, Baylor College of Medicine, Houston, TX 77030, USA; [81]Cell Therapy Institute, Paracelsus Medical University (PMU), 5020 Salzburg, Austria; [82]GeneDx, LLC, Gaithersburg, MD 20877, USA; [83]Texas Children's Hospital, Houston, TX 77030, USA; [84]German Center for Child and Adolescent Health (DZKJ), partner site Hamburg, Hamburg, Germany; [85]Institute of Clinical Human Genetics, University Hospital Regensburg, 93053 Regensburg, Germany
[86]These authors contributed equally
*Correspondence: davor.lessel@klinik.uni-regensburg.de
https://doi.org/10.1016/j.ajhg.2024.12.012.

lymphoma/leukemia 11B, constitutes one example of C2H2-ZnF-containing, DNA-binding transcription factors. As a transcriptional regulator, BCL11B controls various biological processes such as cell death, cell proliferation, and cellular differentiation.[8] Interestingly, due to the specific DNA-binding preferences, the target genes of BCL11B differ among cell types and lineages, thus regulating the gene expression in a context-dependent manner.[9,10] Studies utilizing various genetic manipulations in mice have established pleiotropic functions of Bcl11b in development and differentiation. In the central nervous systems, Bcl11b is involved in the migration, differentiation, and function of neural cells as well as proliferation of neural progenitor cells.[11,12] Bcl11b is necessary for the proper development of the teeth,[13] epidermis,[14] cranium,[15] and white adipose tissue.[16] In the immune system, Bcl11b is involved in the development and maintenance of the T cell lineage[17] and regulation of T cell lineage commitment[18–20] as well as the control of the lineage specification and persistence of type 2 innate lymphoid cells (ILC2s).[21–23] Moreover, mice with a heterozygous loss of Bcl11b are susceptible to thymic lymphomas.[24,25] Notably, 16% of human T cell acute lymphoblastic leukemias carry somatic, inactivating BCL11B variants,[26,27] whereas activating BCL11B genomic rearrangements are potential drivers of lineage-ambiguous leukemias,[28,29] suggesting that BCL11B may act both as a tumor suppressor and an oncogene.

The initial human pathogenic germline BCL11B missense variant was identified in a single individual affected with severe combined immunodeficiency (SCID), neurodevelopmental delay, craniofacial abnormalities, absent corpus callosum, and erythematous psoriaform dermatitis (IMD49 [MIM: 617237]).[30] We subsequently established likely gene-disruptive (LGD) germline variants as a cause of a neurodevelopmental delay with impaired T cell development and severe reduction of ILC2s, which did not result in overt clinical signs of immunodeficiency (IDDSFTA [MIM: 618092]).[31] Since then, more than 50 individuals harboring pathogenic or likely pathogenic BCL11B variants have been documented.[32–47] DNA methylation analysis of peripheral blood obtained from individuals harboring LGD BCL11B variants identified an episignature of high sensitivity and remarkable specificity,[44] consistent with BCL11B being a transcription factor. However, the molecular mechanisms underlying the associated clinical heterogeneity remain mostly elusive.

Here, we describe 39 previously unreported individuals who harbor heterozygous pathogenic or likely pathogenic BCL11B variants and compare their findings to 53 previously documented ones. Integrative analysis of the genotype-phenotype correlations, immune phenotyping, analysis of chromatin immunoprecipitation DNA-sequencing (ChIP-seq) data, dual-luciferase reporter assays, and molecular modeling suggest that, based on the location and nature of the BCL11B alteration, the affected individuals can be categorized in at least three clinical subtypes.

## Material and methods

### Human subjects and genetic analyses

Written informed consent for all 39 affected individuals included in this study was obtained from the parents or legal guardians in accordance with protocols approved by the respective ethics committees of the institutions involved in this study. Next-generation-sequencing-based analyses were performed in various independent research or diagnostic laboratories worldwide using previously described procedures,[31,48–52,53] as described in the supplemental information. Classification of the identified variants was based on the American College of Medical Genetics and Genomics (ACMG) guidelines.[54] For all 39 individuals, clinical data and information on genetic testing were uniformly obtained from attending physicians using a structured clinical summary (supplemental information) and clinical table (Table S1).

### Immunophenotyping

Processing and analysis of blood samples of individuals harboring a heterozygous BCL11B variant followed previously described procedures.[31] In brief, 75 μL of whole blood was incubated with combinations of the following fluorochrome-conjugated antibodies for 30 min at room temperature: the "T-regulatory" panel contained anti-CD3 BV510 (clone: OKT3), anti-CD4 AF700 (clone: OKT4), anti-CD8 BV605 (RPA-T8), anti-CD25 BV421 (clone: 96 BC), anti-CD31 APC-Cy7 (clone: WM59), anti-CD39 PE-Cy7 (A1), anti-CD45RA PE-Dazzle (clone: HI100), anti-CD73 PE (clone: AD2), anti-CD127 BV650 (clone: WM59), anti-HLA-DR BV711 (clone: L243), and anti-CCR4 PerCP-Cy-5.5 (clone: TG6); the "T-invariant" panel contained anti-CD3 BV510 (clone: OKT3), anti-CD4 PE-Dazzle (clone: RPA-T4), anti-CD8 AF700 (clone: HIT8a), anti-CD25 BV421 (clone: 96 BC), anti-CD27 BV650 (clone: O323), anti-CD45RO BV785 (clone: UCHL1), anti-CD69 APC-Cy7 (clone: FN50), anti-CD161 BV605 (clone: HP-3G10), anti-CCR6 PerCP-Cy-5.5 (clone: G034E3), anti-CCR7 BV711 (clone: G043H7), anti-Tgd PE-Cy-7 (clone: 11F2), anti-Va7.2 APC (clone: 3C10), anti-Vd1 FITC (clone: TS-1), anti-Vd2 APC (123R3), and anti-Vd9 FITC (IMMU 360); finally, the "T-effector" panel contained anti-CD3 BV785 (clone: OKT3), anti-CD4 APC-Cy-7 (clone: RPA-T4), anti-CD8 BV510 (RPA-T8), anti-CD25 PE (clone: 2A3), anti-CD28 PE-Cy7 (clone: CD28.2), anti-CD38 AF700 (clone: HIT2), anti-CD45RA PE-Dazzle (clone: HI100), anti-CD57 FITC (clone: HCD57), anti-CD95 BV421 (clone: DX2), anti-CD127 BV650 (clone: WM59), anti-CCR7 APC (clone: G043H7), and anti-HLA-DR BV711 (clone: L243). After staining, 1 mL of BD lysing solution was added for lysis of erythrocytes, and stained cells were washed in PBS and resuspended in fluorescence-activated cell sorting (FACS) buffer. Flow-cytometric analysis was performed on an LSR Fortessa (BD Biosciences). Prior to analysis, a spillover spreading matrix was produced, PMT voltages were optimized, and a compensation matrix was calculated. FlowJo software version 10.8.1 (FlowJo, Ashland, OR, USA) was used for manual analysis, using a gating strategy adapted from Sibbertsen et al.[55]

### ChIP-seq analysis

To identify gene targets of BCL11B, we performed extensive analyses of a publicly available ChIP-seq dataset obtained in HEK293 cells (accession ENCODE: ENCSR770PQN), generated by the ENCODE project.[56] Data on the conservative peaks were obtained from the Gene Expression Omnibus (GEO: GSE92041)

bigBed file and ordered by signalValue, i.e., enrichment of signal over input control in the peak. The functional analysis of peaks and gene assignment was performed using the R package ChIPseeker,[57] with default parameters for feature assignment.

## Plasmids

pIRES plasmid containing sequence for full-length Bcl11b wild-type (WT) protein was a kind gift from Prof. Stefan Britsch (Ulm University). To assess BCL11B transcriptional activity, a construct coding for full-length BCL11B WT protein was reinserted from pIRES to pEGFP-N1 by applying restriction digestion with XhoI and AfeI (Thermo Fisher). Digested DNA was separated on 2% agarose gel, and desirable plasmid parts were extracted by a Monarch DNA Gel Extraction Kit (New England Biolabs) following the manufacturer's instructions and ligated with T4 DNA Ligase (New England Biolabs). This, however, produced a STOP codon between protein sequence and EGFP sequence, so additional mutagenesis was performed utilizing a QuikChange II Site-Directed Mutagenesis Kit (Agilent Technologies) producing final pEGFP-N1-BCL11B-WT plasmid coding for full-length BCL11B WT protein with C-terminal EGFP tag. pmRFP-N1 and pEGFP-N1-BCL11B-WT were subjected to another restriction digestion with XhoI and HpaI (Thermo Fisher), gel separation, gel extraction, and T4 DNA ligase ligation. Subsequently, the EGFP tag sequence was substituted with mRFP, producing a construct coding for full-length BCL11B WT with a C-terminal mRFP tag, respectively. Missense and frameshift variants were then introduced into the BCL11B WT construct by applying the QuikChange II Site-Directed Mutagenesis Kit with specially designed primers (all primer pairs are available upon request). The correctness of the DNA sequence was verified by direct Sanger sequencing as previously described.[58]

Further, primary reporter plasmids containing distal enhancer-like signature (dELS) sequences within SHANK3 (MIM: 606230), LTBP3 (MIM: 602090), and LTBP4 (MIM: 604710) loci were obtained by amplification with primers (all primer pairs are available upon request) designed to amplify the respective genomic regions from DNA isolated from an unaffected individual. Fresh PCR products were inserted in the pCRTM2.1-TOPO vector (Invitrogen) using a TOPO TA Cloning Kit (Invitrogen) following the manufacturer's instructions. Following restriction digestion with KpnI and XhoI (Thermo Fisher), DNA gel separation, and DNA extraction, inserts were ligated into pGL3-Enhancer vector with a modified coding region for firefly luciferase (Promega). Additionally, pNL1.1.PGK [Nluc/PGK] vector (Promega) was used as a transfection normalization control.

## Luciferase assay

HEK293T cells were transfected 24 h after seeding. A master mix with a primary reporter pGL3-Firefly luciferase plasmid (containing a dELS within either SHANK3, LTBP3, or LTBP4) and pNL1.1.PGK [Nluc/PGK] plasmid was combined in serum-free medium and aliquoted. Each aliquot was then supplemented with either pmRFP-N1 empty control vector, pmRFP-N1-BCL11B-WT, or pmRFP-BCL11B containing one of the selected missense variants. For analyses of potential dominant-negative effect, pEGFP-N1 empty control vector and pEGFP-BCL11B-WT were added in combination. Transfection was carried out for 24 h using Turbofect transfection reagent (Thermo Fisher). Next day, cells were loosened from plates by PBS supplemented with 10 mM EDTA, and transfected cells (RFP-positive, or both RFP- and GFP-positive cells) were sorted on FACS Aria IIIu (Becton Dickinson). Following sorting, only transfected cells were transferred to white 96-well plates, and the Nano-Glo dual-luciferase reporter assay was carried out following the manufacturer's instructions (Promega). ONE-Glo EX reagent was added to each sample, and the plate was incubated for 10 min at room temperature, shaking on orbital shaker at 300 rpm. Measurement of firefly luminescence activity was performed on a Synergy H1 Microplate reader (BioTek) or a Spark Multimode Microplate Reader (Tecan). An equal volume of NanoDLR Stop & Glo reagent was added to each sample, and the plate was again incubated for 10 min at room temperature, shaking on orbital shaker at 300 rpm, after which Nanoluc activity in the form of luminescence was assessed. Three experiments were carried out for each dELS (at SHANK3, LTBP3, and LTBP4 loci) and for each BCL11B missense variant in comparison to WT and empty vector. Each experiment was normalized to the mean luminescence of measured samples to correct for different order of magnitude between experiments. Statistical significance was calculated by one-way ANOVA with Dunnett correction for multiple comparisons (GraphPad Prism).

## DNA-binding motif prediction

The DNA-binding motif landscape and DNA-binding specificity of BCL11B-WT and the missense variants were analyzed using two modeling approaches: "Interactive PWM predictor"[3,59] and "Zinc finger recognition code."[4]

# Results

## Identification of likely gene-disruptive variants in BCL11B

Twenty-six heterozygous, pathogenic, or likely pathogenic BCL11B variants have so far been documented in the literature (Figure 1, upper panel). Here, we report 39 individuals, 30 of whom harbor previously unreported heterozygous variants in BCL11B. Among them, 22 individuals harbor a likely gene-disruptive (LGD) germline variant, out of which 11 have so far not been documented in the literature. Unrelated individuals 1 and 2 harbor an identical de novo nonsense variant, NM_138576.3: c.183_189delTCAAATG, p.Cys61*, located in exon 2, predicted to activate the nonsense-mediated mRNA decay and to result in haploinsufficiency. Individuals 3–22 harbor heterozygous frameshift variants located in the last exon (exon 4), which are predicted to escape nonsense-mediated mRNA decay and result in a protein with loss of at least the last two C-terminal DNA-binding zinc-finger domains, C2H2-ZnF5 and C2H2-ZnF6 (Figure 1, lower panel; Table S1). Interestingly, individual 4 harbors a de novo c.1474delC, p.Leu492Serfs*71 variant, which she transmitted to her similarly affected son (individual 5). Siblings, individuals 21 and 22, harbor c.2499delC, p.Cys833Trpfs*11, which was not identified in any of the parental samples, pointing to a gonadal mosaicism. Moreover, we identified five recurrent frameshift variants: c.1552delC, p.Arg518Alafs*45, c.1887_1893delCGGCGGG, p.Gly630Thrfs*91, c.1944_1965delCGGCGCGGTCAACGGGCGCGGG, p.Gly649Alafs*67, c.2448_2461delGAGCCACACCGGCG, p.Ser817Alafs*63, and c.2439_2452dupGCACCGGCGGAGCC, p.His818Argfs*31 (Figure 1). Out of
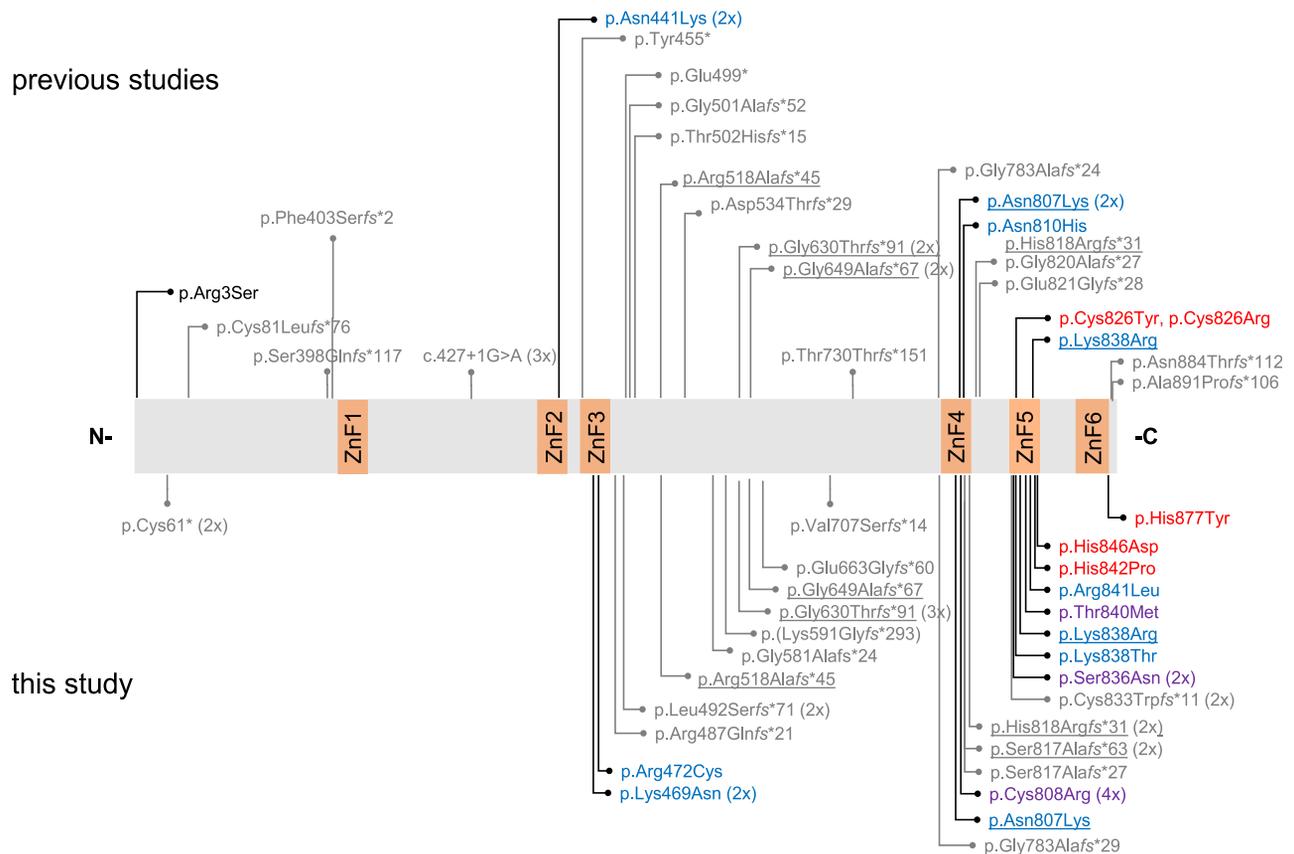
**Figure 1. Locations of identified *BCL11B* germline variants**
Schematic protein structure of BCL11B. Previously identified variants are shown in the upper panel. Variants identified in this study are shown in the lower panel. Likely gene-disruptive (LGD) variants are shown in gray. Missense variant in the very N terminus is shown in black. Missense variants affecting "specificity residues" are shown in blue, other missense variants within the α helix are shown in violet, and missense variants affecting ZnF-contacting cysteines and histidines are shown in red. Recurring variants are underlined. C, C terminus; N, N terminus; ZnF, zinc-finger C2H2 domain.

the identified *BCL11B* LGD variants, only the c.1742delG, p.Gly581Ala*fs*\*24, with allele frequency of 0.000003, is present in the gnomAD dataset v.4.1.0[60] (Table S1). *BCL11B*, with a probability of loss-of-function intolerance (pLI) score of 1 and a loss-of-function observed/expected upper bound fraction (LOEUF) score of 0.27, is strongly intolerant to loss-of-function variants. Thus, according to The ACMG guidelines,[54] all variants were classified as either likely pathogenic or pathogenic (Table S1).

### Identification of *BCL11B* missense variants affecting DNA-binding zinc-finger domains

C2H2-ZnFs harbor a two-stranded antiparallel β sheet and one DNA-contacting α helix, which regulates DNA binding and sequence preference. The stability of C2H2-ZnFs is provided by the zinc-binding cysteine and histidine residues.[2] Here, we identified 17 individuals harboring a heterozygous amino acid substitution affecting either one of the residues within the DNA-contacting α helix or one of the zinc-binding residues within one of the BCL11B's C2H2-ZnF. Among them, three individuals harbor a missense variant within C2H2-ZnF3. Individuals 23 and 24 harbor different *de novo* nucleotide substitutions, namely c.1407G>T and

c.1407G>C, respectively that, however, result in identical amino acid substitution p.Lys469Asn. Individual 25 harbors a *de novo* c.1414C>T, p.Arg472Cys variant. Two missense variants were identified within C2H2-ZnF4, one of them previously reported (individual 26, with a *de novo* c.2421C>G, p.Asn807Lys variant).[31,38] Individuals 27–29 inherited a c.2422T>C, p.Cys808Arg from their similarly affected father (individual 30), in whom the variant occurred *de novo*. We found seven missense variants in C2H2-ZnF5. Individuals 31 and 32 harbor the identical *de novo* c.2507G>A, p.Ser836Asn variant. Two individuals harbor an amino acid substitution affecting Lys838, individual 33 harboring a *de novo* c.2513A>C, p.Lys838Thr variant and individual 34 a *de novo* c.2513A>G, p.Lys838Arg variant. Notably, an identical *de novo* p.Lys838Arg variant was recently reported.[35] Further, *de novo* variants c.2519C>T, p.Thr840Met, c.2522G>T, p.Arg841Leu, c.2525A>C, p.His842Pro, and c.2536C>G, p.His846Asp were identified in individuals 35, 36, 37, and 38, respectively. Finally, we identified a single missense variant within C2H2-ZnF6, a *de novo* variant c.2629C>T, p.His877Tyr in individual 39 (Figures 1 and 2).

Notably, six of the identified missense variants within ZnF-C2H2s affected one of the four (−1, +2, +3, and +6)
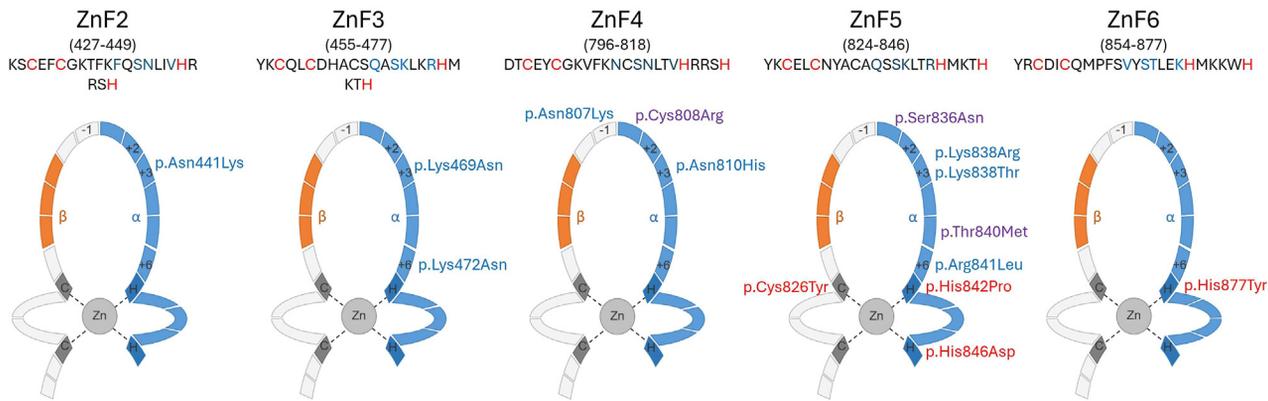
**Figure 2. Location of missense variants within BCL11B's Cys2-His2 zinc-finger domains**

Schematic diagrams of Cys2-His2 (C2H2-ZnF) zinc-finger domains 2–6. Each C2H2-ZnF contains paired cysteines (C) and histidines (H) that bind the zinc ion (Zn). β sheet is depicted in orange, α helix is depicted in blue, and 1, +2, +3, and +6 depict "specificity residues" within the α helix. Missense variants affecting "specificity residues" are shown in blue, other missense variants within the α helix are shown in violet, and missense variants affecting ZnF-contacting cysteines and histidines are shown in red.

critical C2H2-ZnF "specificity residues", that is, variants p.Lys469Asn, p.Arg472Cys, p.Asn807Lys, p.Lys838Thr, p.Lys838Arg, and p.Arg841Leu (Figure 2). Such missense variants are thought to impair binding of the altered BCL11B to its physiologic target DNA sites and additionally promote binding to alternative DNA-binding sites.[31] Three missense variants, p.Cys808Arg, p.Ser836Asn, and p.Thr840Met, are localized within ZnF-C2H2s, although not affecting one of the four "specificity residues" (Figure 2). We hypothesized that they may have steric effects on the α helix containing the DNA-recognition site, thereby reducing the affinity of the altered protein for binding to its target DNA sites. The last three missense variants, p.His842Pro, p.His846Asp, and p.His877Tyr, affect histidine residues that are in direct contact with the zinc cation (Figure 2), likely unfolding C2H2-ZnF5 and ZnF6-C2H2, respectively, and resulting in loss of function.[2]

None of these *BCL11B* missense variants are present in the gnomAD dataset v.4.1.0 (Table S1),[61] indicating that they are extremely rare and likely to be disease associated variants. Thus, according to The ACMG guidelines,[54] again all these variants were classified as either likely pathogenic or pathogenic (Table S1).

### Clinical spectrum of individuals harboring *BCL11B* likely gene-disruptive variants

All individuals reported here harboring an LGD variant are affected by a neurodevelopmental disorder, albeit with variable expressivity and interfamilial variability (Table 1 and Note S1). In more detail, all individuals have mild to moderate intellectual disability and impaired speech development, and most of them (77%) have a delay in motor development. Further common phenotypic features in this cohort include various dental anomalies (Figure 3), such as dental crowding, dental caries, hypodontia, and oligodontia (71%). Additionally, 68% had feeding difficulties in infancy. Interestingly, a review of the literature revealed both dental anomalies (32%) and feeding diffi-

culties (23%) to be less common in previously documented cases (Table 1). Similar to the previous findings, behavioral issues including attention-deficit/hyperactivity disorder (ADHD), autism spectrum disorder, anxiety, obsessive-compulsive disorder, frustration intolerance, and aggressive behavior were relatively common (67%). Additional common phenotypic features included refractive error (45%) and muscular hypotonia (41%). Common facial dysmorphisms (Table 1 and Figure 3) included prominent nose (68%), thin upper lip vermilion (67%), hypertelorism (64%), long philtrum (59%), thin eyebrows (57%), myopathic facial appearance (45%), and small palpebral fissures (32%). Abnormalities of the skull including craniosynostosis, scaphocephaly (sagittal craniosynostosis), microcephaly, macrocephaly, and dolichocephaly were observed in 11 individuals (58%). Compared to previous studies, hypertelorism, skull abnormalities, and myopathic facial appearance were somewhat more common in our case series (Table 1). Regarding the immune system, 12 (55%) had frequent infections in the first years of life, 12 (55%) developed some type of allergy or atopy, and 7 (33%) had asthma, similar to the previous findings (Table 1). Noteworthy, only a single individual (individual 14) developed a hematologic malignancy, a T cell large granular lymphocytic leukemia.

### Clinical variability in individuals harboring *BCL11B* missense variants within C2H2-ZnFs

Compared to the individuals harboring an LGD variant, we observed high clinical variability among individuals harboring a missense variant within the C2H2-ZnFs (Table 2 and Note S1), likely due to variant-specific effects. Individuals 23 and 24, both harboring a *de novo* p.Lys469Asn variant, were affected by neonatal-onset multisystem anomalies. These included common dysmorphic features, sparse hair, global developmental delay (GDD), muscular hypotonia, oral feeding problems, respiratory insufficiency, and early-onset epileptic encephalopathy with

**Table 1.** Summary of clinical signs and symptoms of individuals harboring *BCL11B* likely gene-disruptive (LGD) variants

| Clinical findings | Likely gene-disruptive variants (this study) | Likely gene-disruptive variants (previous studies)[31,33,36,38–41,43–47] | Likely gene-disruptive variants (all studies) |
|---|---|---|---|
| Sex | 15 female/7 male | 22 female/23 male | 37 female/30 male |
| **Cognitive and motor development** | | | |
| Intellectual disability | 21/21 (100%) | 39/43 (91%) | 60/64 (94%) |
| Speech impairment | 22/22 (100%) | 41/43 (95%) | 63/65 (97%) |
| Delay in motor development | 17/22 (77%) | 32/43 (74%) | 49/65 (75%) |
| **Dysmorphic features** | | | |
| Prominent nose | 15/22 (68%) | 28/44 (64%) | 43/66 (65%) |
| Thin upper lip vermilion | 14/21 (67%) | 37/44 (84%) | 51/65 (78%) |
| Hypertelorism | 14/22 (64%) | 17/44 (39%) | 31/66 (47%) |
| Long philtrum | 13/22 (59%) | 31/44 (70%) | 44/66 (67%) |
| Skull abnormalities | 11/19 (58%) | 9/33 (27%) | 20/52 (38%) |
| Thin eyebrows | 12/21 (57%) | 25/44 (47%) | 37/65 (57%) |
| Myopathic facial appearance | 10/22 (45%) | 10/44 (23%) | 20/66 (30%) |
| Small palpebral fissures | 7/22 (32%) | 23/44 (52%) | 30/66 (45%) |
| Retrognathia | 2/22 (9%) | 6/44 (14%) | 8/66 (12%) |
| **Neurologic signs** | | | |
| Behavioral issues | 14/21 (67%) | 23/42 (55%) | 37/63 (59%) |
| Muscular hypotonia | 9/22 (41%) | 6/25 (24%) | 15/47 (32%) |
| Reduced fine motor skills | 7/22 (32%) | 3/16 (19%) | 10/38 (26%) |
| Brain MRI anomalies | 3/10 (30%) | 10/33 (30%) | 13/43 (30%) |
| Gait abnormalities | 5/21 (24%) (1 non-ambulatory) | 2/15 (13%) | 7/36 (19%) |
| Seizures | 3/22 (14%) | 3/40 (8%) | 6/62 (10%) |
| Dystonia | 2/22 (9%) | 1/14 (7%) | 3/36 (8%) |
| Involuntary movements | 1/22 (4.5%) | 0/14 | 1/36 (3%) |
| Cerebral palsy | 1/22 (4.5%) | 1/14 (7%) | 2/36 (6%) |
| Hyperkinesia | 1/23 (4%) | 0/14 | 1/37 (3%) |
| **Other** | | | |
| Dental anomalies | 15/21 (71%) | 14/44 (32%) | 29/65 (45%) |
| Feeding difficulties | 15/22 (68%) | 5/22 (23%) | 20/44 (45%) |
| Refractive error | 10/22 (45%) | 13/37 (35%) | 23/59 (39%) |
| Short stature | 7/19 (37%) | 4/34 (12%) | 11/53 (21%) |
| Clinodactyly | 5/22 (23%) | 1/14 (7%) | 6/36 (17%) |
| Hypothyroidism | 3/22 (14%) | 2/32 (6%) | 5/54 (9%) |
| Hair abnormalities | 3/22 (14%) | 1/41 (2%) | 4/63 (6%) |
| **Immune system function** | | | |
| Frequent infections | 12/22 (55%) | 22/44 (50%) | 34/66 (52%) |
| Allergies | 12/22 (55%) | 6/20 (30%) | 18/42 (43%) |
| Asthma | 7/21 (33%) | 11/38 (29%) | 18/59 (31%) |
| Hematologic malignancy | 1/22 (4.5%) | 0/42 | 1/64 (1.5%) |

**Figure 3. Images of individuals affected by *BCL11B*-associated disorders**

(A) Dental photos show primary molars of individual 8 immediately after eruption (left). The other two photos were taken at the age of 9 years. The "raised" gums above the left incisor were much more pronounced after the permanent tooth erupted and have slowly but steadily grown well downward.

(B) Images of individual 10 at the age of 5 years shows short forehead, thin eyebrows, "beaked nose" with narrow nasal tip, small mouth, horizontal crease of chin, bilateral earlobe hypoplasia, and clinodactyly of II toe and V finger bilaterally (right panel).

(C) Images of individual 12 at the age of 5 years show a high anterior hairline, small upslanting palpebral fissures, thin eyebrows, a broad forehead, a short nose with anteverted nostrils, a long philtrum, and small mouth with thin lips and downturned corners. Note a somewhat short neck with low posterior hairline.

(D) Images of individual 14 at the age of 19 years show upwardly slanted palpebral fissures, epicanthal folds, broad nasal bridge, long nose, downturned nasal tip, short columella, long philtrum, and thin upper vermillion.

(E) Images of individual 15 at the age of 12 years show a high anterior hairline, a long nose with protruding columella hypoplastic alae nasi, thin upper lip vermilion, and low-set ears.

(F) Images of individual 18 at the age of 3 years show midface flattening, flattened nasal bridge with rounded nasal tip, micrognathia, and a small mouth.

(G) Images of individual 23 at the age of 20 months show a high anterior hairline, white and thin hair, absent eyelashes, small mouth, and micrognathia.

and epileptic encephalopathy with global neurologic regression. Individual 26 had GDD but did not develop congenital erosive dermatitis, which we previously observed in an individual harboring the identical *de novo* p.Asn807Lys variant.[31]

The four affected family members harboring the p.Cys808Arg variant (individuals 27–30) showed interfamilial clinical variability. Twins (individuals 27 and 28) exhibited moderate delay in speech and motor development, poor fine motor skills, hyperkinetic movement disorder, anxiety, and obsessive-compulsive disorder. Their younger brother (individual 29) had an articulation disorder, severe rigidity dystonia, and ataxic gait. Their father (individual 30) had poor fine motor skills and mild hyperkinetic movement disorder, and developed Henoch-Schonlein purpura in

agenesis or absence of corpus callosum. Abnormalities of the skin included pigmentary mosaicism in individual 23 (Figure 3E) and periorbital skin and scalp eczema in individual 24. Both had an idiopathic CD4$^+$ T cell lymphocytopenia (ICL) and died following infections in the third and second year of life, respectively. Individual 25, who harbors a *de novo* p.Arg472Cys variant, had developmental

**Table 2.   Clinical signs and symptoms of individuals harboring pathogenic *BCL11B* missense variants within Cys2-His2 zinc-finger domains (C2H2-ZnF)**

| Location of *BCL11B* missense variants | Affecting a "specificity residue" within a C2H2-ZnF | | | | | | | | Within a C2H2-ZnF but not affecting a "specificity residue" | | | Within a C2H2-ZnF, affecting a zinc-binding cysteine or histidine residue | |
|---|---|---|---|---|---|---|---|---|---|---|---|---|---|
| Exact *BCL11B* missense variants | Asn441Lys | Lys469Asn | Arg472Cys | Asn807Lys1 | Asn810His | Lys838Thr | Lys838Arg1 | Arg841Leu | Cys808Arg | Ser836Asn | Thr840Met | Cys826Tyr | His842Pro |
| | | | this study | this study | | this study | this study | this study | this study | this study | this study | Cys826Arg | His846Asp |
| | | | | | | | | | | | | | His877Tyr |
| | | | | | | | | | | | | | this study |
| Sex | 2M[30,32] | 1F/1M | 1F | 2F[31,38]/1M[31,38] | 1F[36] | 1M | 1F[35]/1M | 1M | 4M | 1F/1M | 1M | 1F[37]/1M[44] | 1F/2M |
| **Cognitive and motor development** | | | | | | | | | | | | | |
| Intellectual disability | 1/1 | 2/2 | + | 2/2 | + | + | 2/2 | + | 0/4 | 1/2 | + | 2/2 | 3/3 |
| Speech impairment | 1/1 | 2/2 | + | 2/2 | + | + | 2/2 | + | 3/4 | 2/2 | − | 1/1 | 3/3 |
| Delay in motor development | 1/1 | 2/2 | + | 3/3 | + | + | 2/2 | + | 2/4 | 2/2 | − | 1/1 | 3/3 |
| **Dysmorphic features** | | | | | | | | | | | | | |
| Prominent nose | 2/2 | 0/2 | − | 1/3 | + | + | 0/2 | + | 0/4 | 2/2 | + | 1/1 | 0/3 |
| Thin upper lip vermilion | 0/1 | 2/2 | + | 2/3 | + | + | 1/2 | + | 3/4 | 2/2 | − | 1/1 | 2/3 |
| Hypertelorism | 1/2 | 1/2 | + | 2/3 | + | − | 1/2 | + | 0/4 | 2/2 | − | 0/1 | 1/3 |
| Long philtrum | 2/2 | 0/2 | + | 1/3 | + | + | 1/2 | + | 2/4 | 1/2 | − | 0/1 | 1/3 |
| Skull abnormalities | 2/2 | 2/2 | + | 1/3 | − | + | 0/2 | − | 0/4 | 2/2 | + | 1/2 | 2/3 |
| Thin eyebrows | 2/2 | 0/2 | + | 0/3 | + | − | 0/2 | − | 0/4 | 0/2 | + | 1/1 | 0/3 |
| Myopathic facial appearance | 0/2 | 0/2 | − | 2/3 | + | + | 2/2 | + | 0/4 | 0/2 | − | 0/1 | 1/3 |
| Small palpebral fissures | 2/2 | 0/2 | − | 2/3 | + | − | 0/2 | + | 0/4 | 1/2 | − | 0/1 | 1/3 |
| Retrognathia | 2/2 | 2/2 | + | 0/3 | − | − | 0/2 | + | 0/4 | 1/2 | + | N/A | 0/3 |
| **Neurologic signs** | | | | | | | | | | | | | |
| Behavioral issues | ? | ? | ? | 0/2 | ? | ? | 0/2 | + | 2/4 | 0/2 | + | 0/1 | 3/3 |
| Muscular hypotonia | 2/2 | 2/2 | + | 2/2 | − | + | 2/2 | + | 3/4 | 2/2 | − | N/A | 1/3 |
| Reduced fine motor skills | ? | ? | + | 0/2 | N/A | N/A | N/A | − | 3/4 | 0/2 | + | N/A | 0/3 |
| Brain MRI anomalies | 2/2 | 2/2 | + | 1/2 | N/A | + | 1/1 | N/A | 1/1 | 0/2 | − | 0/2 | 2/3 |
| Gait abnormalities | 1/1 | ? | + | 2/3 | + | + | 2/2 | − | 4/4 | 2/2 | − | N/A | 0/3 |
| Seizures | 1/1 | 2/2 | + | 0/2 | N/A | + | 0/2 | − | 0/4 | 0/2 | − | 0/1 | 0/3 |
| Dystonia | 1/1 | ? | ? | 0/2 | N/A | − | 2/2 | − | 3/4 | 0/2 | − | N/A | 0/3 |
| Involuntary movements | N/A | ? | + | 0/2 | N/A | − | 2/2 | − | 0/4 | 0/2 | + | N/A | 0/3 |

(*Continued on next page*)

**Table 2.** *Continued*

| Location of *BCL11B* missense variants | Affecting a "specificity residue" within a C2H2-ZnF | | | | | | | | Within a C2H2-ZnF but not affecting a "specificity residue" | | | Within a C2H2-ZnF, affecting a zinc-binding cysteine or histidine residue | |
|---|---|---|---|---|---|---|---|---|---|---|---|---|---|
| Cerebral palsy | N/A | ? | + | 1/3 | N/A | + | 2/2 | – | 0/4 | 0/2 | – | N/A | 0/3 |
| Hyperkinesia | N/A | ? | N/A | 0/2 | N/A | N/A | N/A | – | 3/4 | 0/2 | – | N/A | 0/3 |
| **Other** | | | | | | | | | | | | | |
| Feeding difficulties | 1/1 | 2/2 | – | 2/3 | + | + | 1/2 | – | 1/4 | 2/2 | – | 1/1 | 2/3 |
| Dental anomalies | 1/2 | 1/2 | – | 3/3 | + | – | 0/2 | N/A | 2/4 | 1/2 | – | 0/1 | 1/3 |
| Refractive error | 1/1 | 1/1 | – | 0/3 | N/A | + | 0/2 | – | 0/4 | 0/2 | – | 0/1 | 2/3 |
| Short stature | N/A | 1/1 | – | 0/2 | N/A | + | 1/1 | N/A | 0/4 | 0/2 | – | N/A | 1/3 |
| Clinodactyly | N/A | 0/2 | – | 0/3 | N/A | – | 0/2 | – | 0/4 | 0/2 | – | N/A | 0/3 |
| Hypothyroidism | N/A | 0/2 | – | 0/3 | N/A | – | 0/2 | – | 0/4 | 0/2 | – | 0/1 | 0/3 |
| Hair abnormalities | N/A | 2/2 (sparse) | – | 0/3 | – | – | 0/2 | – | 0/4 | 0/2 | – | 1/1 | 0/3 |
| **Immune system function** | | | | | | | | | | | | | |
| Immune response anomalies | 1 SCID | 2/2 | – | 1/3 | SCID | SCID | 2/2 | + | 4/4 | 2/2 | – | 1/2 | 1/3 |
| | 1 ICL | ICL | | | | | (1 ITP) | | FI | FI | | FI | FI |
| Allergies | N/A | 1/1 | – | 1/3 | N/A | – | 0/2 | + | 0/4 | 0/2 | – | 1/2 | 2/3 |
| Asthma | N/A | 0/1 | – | 1/3 | N/A | – | 0/2 | + | 0/4 | 1/2 | – | 2/2 | 0/3 |
| Hematologic malignancy | N/A | 0/2 | – | 0/3 | N/A | – | 0/2 | – | 0/4 | 1/2 | – | NA | 0/3 |

F, female; M, male; +, present; –, absent; ?, too young to evaluate; N/A, unknown; SCID, severe combined immunodeficiency; ICL, idiopathic CD4$^+$ T cell lymphocytopenia; ITP, idiopathic thrombocytopenic purpura; FI, frequent infections.

adulthood. All family members suffered from frequent viral infections and/or environmental allergies (Table 2 and Note S1). Individuals 31 and 32 harbor the identical *de novo* p.Ser836Asn variant, had GDD, and had a history of frequent infections. Notably, individual 32 developed acute T cell lymphoblastic leukemia at the age of 12 years. Individual 33, harboring a *de novo* p.Lys838Thr variant, had severe GDD with focal seizures, dysgenesis of the corpus callosum, cortical vision loss, and SCID. Individual 34, harboring a heterozygous p.Lys838Arg variant, was affected with severe GDD, was non-ambulatory, and had no speech at the age of 24 years, with spastic cerebral palsy, abnormal involuntary movements, thrombocytopenia purpura, and a history of frequent infections. Following an unremarkable early development, individual 35, who harbors a *de novo* p.Thr840Met variant, starting from the age of 4 years developed mild intellectual disability, developmental coordination disorder, ADHD, and subcortical myoclonias. Individual 36, harboring a *de novo* p.Arg841Leu variant, had GDD, autistic features, food allergies, asthma, and a mild decrease of T cell counts. Individual 37, harboring a *de novo* p.His842Pro variant, was affected by GDD, lingual dyspraxia, and asthma. Individual 38, harboring a *de novo* p.His846Asp variant, had GDD with autistic features, food allergies, and asthma. Lastly, individual 39, harboring a *de novo* p.His877Tyr variant, was affected by GDD with autistic features. Notably, all individuals harboring a missense variant displayed variable dysmorphic features, as summarized in Table 2.

### Common immune traits in individuals with *BCL11B* variants

Analyses in mice have established Bcl11b as essential for the development of T cells and the specification and maintenance of ILC2s.[17–23] In line with murine data, we have previously observed alterations in the T cell compartment and severe reduction of ILC2s in individuals harboring pathogenic, mostly LGD, *BCL11B* variants.[31] Thus, to further delineate the *BCL11B*-associated immune phenotype, we analyzed the immune compartment of 13 available affected individuals included in this study. Six individuals (individuals 2, 6, 8, 9, 14, and 15) harbored an LGD variant, and seven (individuals 25, 27, 28. 29, 31, 32, and 35) harbored a missense variant. Similar to our previous findings, leukocyte counts were mostly within the normal range (data not shown). Furthermore, six out of nine individuals analyzed had high eosinophil counts, in line with increased prevalence of allergy/atopy (Table S2). The absolute count and frequency of T cells was within the normal range in all individuals, except individual 31 who had few T cells, and the two cases with malignancies (individuals 13 and 32) with aberrant lymphocyte cell compartment due to the tumor (T cell large granular lymphocytic) and chemotherapy, respectively. The frequency of B and natural killer cells was also within normal range, except in individuals with a malignancy (individuals 14 and 32). Detailed analysis of the T cell compartment revealed an over-representation of cells bearing the T-$\gamma\delta$ receptor in 10 out of 12 individuals without a malignancy and an abnormally low percentage of $CD4^+$ recent thymic emigrants (RTEs), that is, the cells that have recently migrated from the thymus to the peripheral blood, indicating impaired T-$\alpha\beta$ cell development, in nine individuals (Table S2). As a result, most of the individuals with few RTEs also had a low frequency of naive $CD4^+$ cells and $CD8^+$ T cells and a concomitant higher frequency of memory T cells (data not shown). Interestingly, although we previously suggested that the reduction of ILC2s is pathognomonic for *BCL11B*-associated disorders, in this cohort we observed a low proportion of ILC2s in only eight individuals. Of note, the reduction in the frequency of ILC2s occurred in all analyzed individuals harboring an LGD *BCL11B* variant and both individuals harboring p.Ser836Asn. In contrast, family members (individuals 27–29) who harbor p.Cys808Arg, and individuals 25 and 35 who harbor p.Arg472Cys or p.Thr840Met, respectively, had ILC2s within the normal range (Table S2). Taken together, our data show that T cell development is affected in nearly all analyzed individuals and indicate low thymic output and a bias in the usage of the T cell receptor chains. In contrast, the ILC2 compartment seems to be altered in a variant-specific manner, primarily in individuals harboring LGD variants.

### *BCL11B* ZnF-C2H2 missense variants differentially affect binding to target genes

To further confirm the pathogenicity of the here identified ZnF-C2H2 missense variants and possibly provide an explanation for the variability in clinical and immune phenotype, we next analyzed the publicly available ChIP-seq (ChIP with massively parallel DNA sequencing) dataset obtained in HEK293 cells (accession ENCODE: ENCSR770PQN) generated by the ENCODE project.[56] Using the ChIPseeker package,[57] we annotated 9,009 conservative peaks. The full list including annotation with peaks ordered by descending signal value (i.e., enrichment of signal over input control) can be found in Table S3. Notably, almost half of the peaks, 4,123 (46%), were located within 1 kb each side of an annotated transcription start site (TSS) (Figure S1). To analyze whether the ZnF_C2H2 missense variants affect the DNA-binding affinity, we chose three putative binding targets, each affecting a candidate *cis*-regulatory element (cCRE),[62] namely, a dELS within *SHANK3* (ENCODE: EH38E2173377), a dELS within *LTBP3* (ENCODE: EH38E1545299), and a dELS within *LTBP4* (ENCODE: EH38E1954213) (Figure S2). Significantly stronger luciferase activity for the three target dELS in HEK293T cells transfected with a plasmid encoding WT human BCL11B compared to those transfected with the empty vector confirmed the binding to all three targets (Figure 4A). We next measured the transcriptional activity of the three missense variants within a C2H2-ZnF that do not affect a "specificity residue," p.Cys808Arg, p.Ser836Asn, and p.Thr840Met, and of four missense
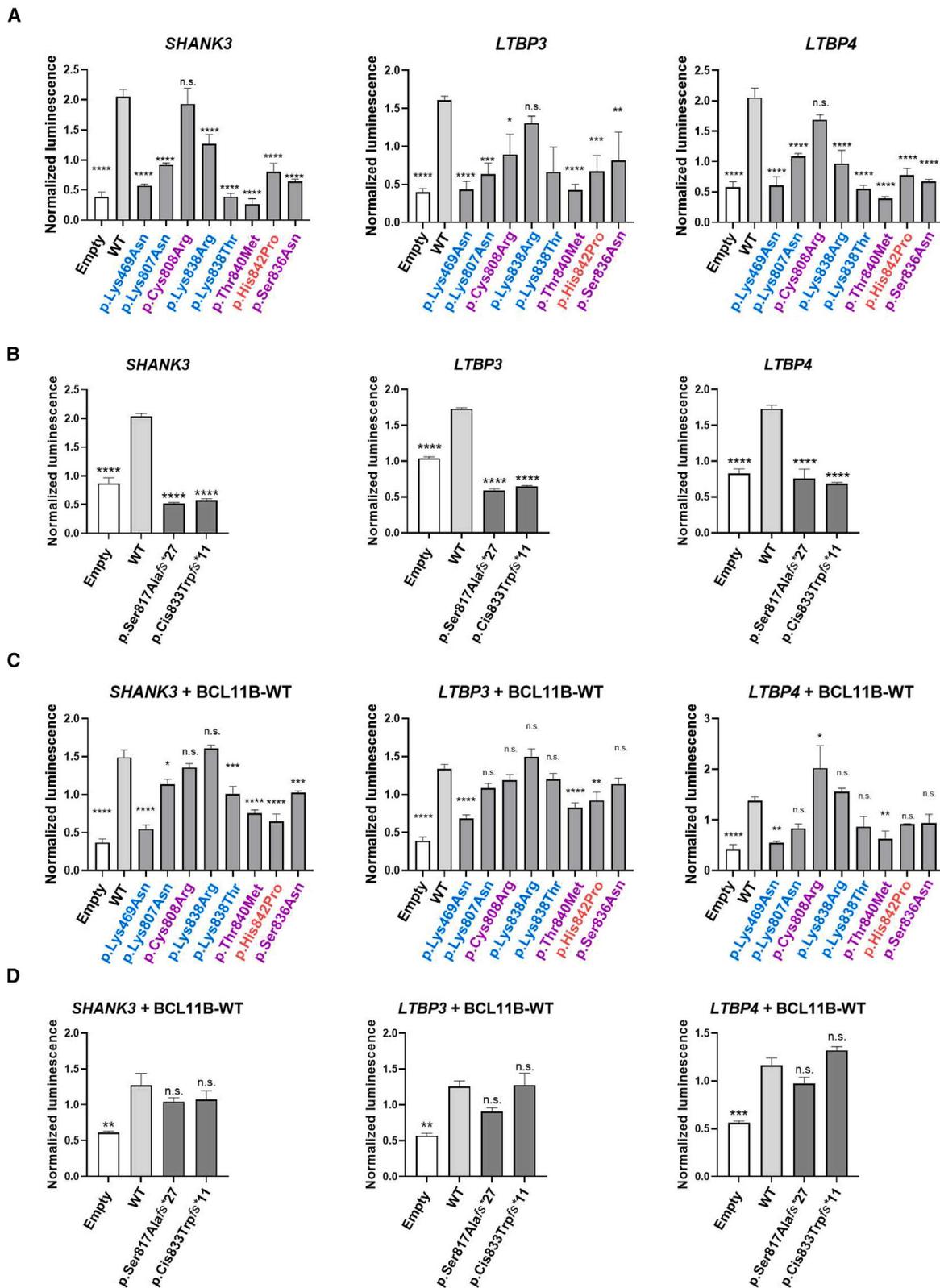
**Figure 4. Analysis of DNA-binding affinity of selected *BCL11B* missense variants**

Luciferase assay utilizing HEK293T cells.

(A) Firefly luciferase plasmid (containing a dELS within either *SHANK3*, *LTBP3*, or *LTBP4* locus) and pNL1.1.PGK [Nluc/PGK] plasmid were transfected together with empty pRFP-N1, pRFP-N1-*BCL11B*-WT, or one of the depicted missense variants in pRFP-N1-*BCL11B* plasmid. Results are presented as the means from three independent experiments. Each experiment was normalized to the mean luminescence of measured samples to correct for different order of magnitude between experiments.

(B) Experiments as in (A) performed for selected frameshift variants.

variants affecting a "specificity residue" within a C2H2-ZnF, p.Lys469Asn, p.Asn807Lys, p.Lys838Thr, and p.Lys838Arg along with p.His842Pro, affecting a zinc-binding histidine residue within C2H2_ZnF5. For the analysis of the p.Lys469Asn variant, we introduced only the nucleotide substitution c.1407G>T as identified in individual 23. The measurement of the luciferase activity revealed that all mutant proteins, apart from p.Ser836Asn and p.Cys808Arg, displayed significantly reduced activation for each of the analyzed targets compared to the WT. The p.Ser836Asn showed decreased activation at the *SHANK3* and *LTBP4* loci, while p.Cys808Arg only showed this at the *LTBP3* locus (Figure 4A). To compare the findings obtained by analyzing missense variants to proteins lacking C-terminal C2H2-ZnFs, we next analyzed two frameshift variants that were identified in affected individuals. p.Ser817Ala*fs*\*27, which alters the amino acid sequence of the C2H2-ZnF4, likely results in a truncated protein lacking the last two C2H2-ZnFs, and p.Cys833Trp*fs*\*11, which alters the amino acid sequence of C2H2-ZnF5, likely results in a truncated protein lacking the last C2H2-ZnF6. Notably, both frameshift variants, to a similar degree, displayed significantly reduced activation for each of the analyzed targets compared to the WT (Figure 4B).

We next assessed whether any of the missense variants exert a dominant-negative effect. When each of the mutants was co-transfected with the WT BCL11B vector, we observed differing results. Co-expression of p.Cys808Arg and p.Ser836Asn did not inhibit WT activation for any of the three targets. Mutants p.Asn807Lys, p.Lys838Arg, and p.His842Pro inhibited WT activation only at the *SHANK3* locus, and p.Thr840Met inhibited WT activation at *SHANK3* and *LTBP3* loci, whereas p.Lys469Asn and p.Lys838Thr inhibited WT activation for all three targets, albeit to a different degree. Thus, these data suggest that specific ZnF-C2H2 missense variants exert a dominant-negative effect in a target-dependent manner (Figure 4C). To further evaluate whether this dominant-negative effect is specific for missense variants, we repeated the experiments analyzing the two frameshift variants, p.Ser817Ala*fs*\*27 and p.Cys833Trp*fs*\*11. Notably, their co-expression did not inhibit WT activation for any of the three targets, suggesting that they do not exert a dominant-negative effect (Figure 4D).

### Missense *BCL11B* variants affecting ZnF-C2H2 specificity residues are predicted to regulate alternative genome regions

Transcriptional regulation governed by C2H2-ZnF-containing proteins is not only dependent on DNA-binding affinity but also on their specificity. The latter is mainly controlled by the four "specificity residues" that are the most exposed amino acids on the surface of the DNA-contacting α helix.[2] We have previously postulated that *BCL11B* missense variants affecting a "specificity residue" within a C2H2-ZnF may cause clinical heterogeneity through acquisition of alternative DNA-binding regions.[31] Accordingly, the affected individuals presented here who harbor a *BCL11B* missense variant affecting a "specificity residue" displayed a broader and more severe phenotype compared to other individuals harboring *BCL11B* variants. However, this clinical variability could not be explained by differential binding affinity in our assays (Figure 4). We therefore utilized two independent bioinformatics algorithms, "Zinc Finger Recognition Code"[4] and "Interactive PWM predictor,"[3,59] to analyze the DNA-binding preferences of the *BCL11B* missense variants within C2H2-ZnFs. Importantly, none of the other C2H2-ZnF missense variants within the DNA-contacting α helix were predicted to regulate alternative targets, suggesting that their main mode of action is the reduced binding capacity due to steric effects on the α-helix-containing DNA-recognition site. In contrast, both modeling approaches, albeit in a different manner, suggest that all missense variants affecting a "specificity residue" result in binding to different alternative genomic sequences, thereby probably regulating different alternative target genes (Figures 5 and S3) and providing further clarification of the observed clinical heterogeneity.

## Discussion

This study further delineates the clinical spectrum of *BCL11B*-related neurodevelopmental disorders through analysis of 92 affected individuals, 39 of whom have so far not been reported in the literature. All affected individuals display impaired function of the nervous system, ranging from severe GDD to poor fine motor skills and late-onset, mild hyperkinetic movement disorder. Most individuals display impaired development of the immune system, although overt signs of immunodeficiency are observed exclusively in individuals harboring missense variants affecting "specificity residues" within the DNA-contacting α helices. In line with previous findings in mice,[13–15] further commonly affected organs include the cranium, skin, and teeth. Based on the clinical, genetic, and molecular findings, we propose that *BCL11B* alterations result in a phenotypic spectrum that can be classified into at least three subtypes.

Individuals harboring heterozygous LGD *BCL11B* variants are affected by mild to moderate intellectual disability and impaired speech development, and the majority

(C) For analyses of potential dominant-negative effect, pEGFP-*BCL11B*-WT was added in combination with the above. Statistical significance was calculated by one-way ANOVA with recommended Dunnett correction for multiple comparisons (GraphPad Prism). Means ± standard deviation values are based on three independent experiments. Significantly different from *BCL11B*-WT: \**p* < 0.05, \*\**p* < 0.01, \*\*\**p* < 0.001, \*\*\*\**p* < 0.0001; n.s., not significantly different from *BCL11B*-WT.
(D) Experiments as in (C) performed for selected frameshift variants.
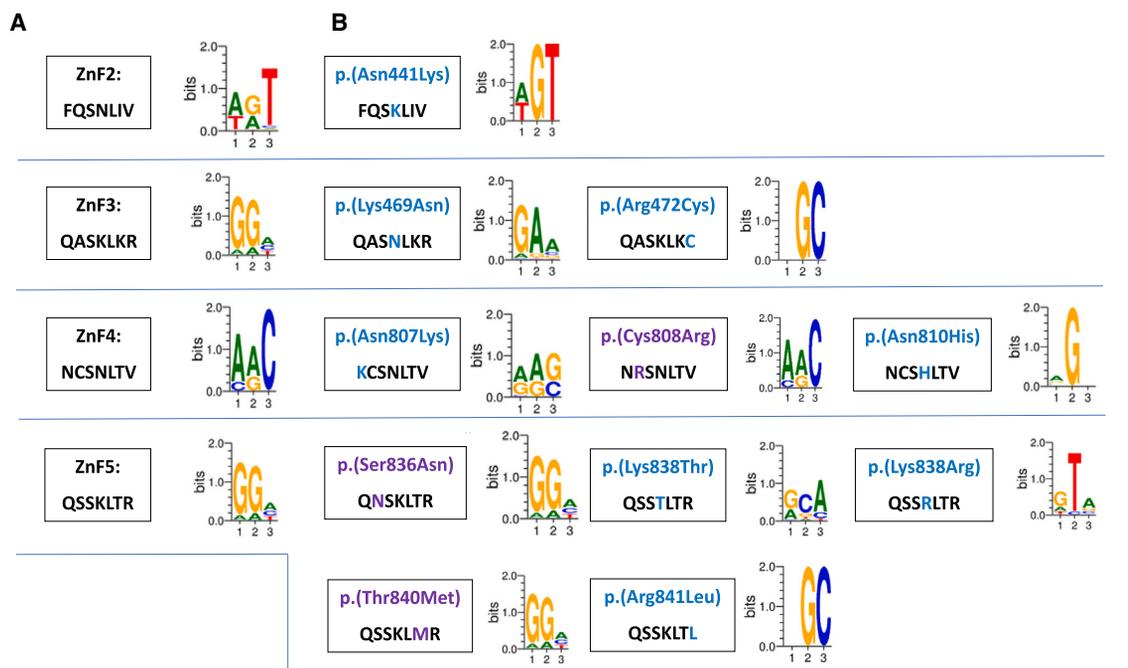
**Figure 5. Modeling of BCL11B DNA-binding specificity due to *BCL11B* missense variants**
(A) Predicted DNA-binding sites of the BCL11B-WT for the four C2H2-ZnFs in which missense variants were identified.
(B) Predicted DNA-binding sites for each of the missense variants within the α helix. Note that all missense variants affecting a "specificity residue" (shown in blue) alter the DNA-binding site and are therefore predicted to bind to different alternative genomic sequences as compared to the *BCL11B*-WT. Missense variants within the α helix not affecting a "specificity residue" (shown in violet) do not alter the DNA-binding specificity. Data are based on "Interactive PWM Predictor."[3]

display a delay in motor development. Further common clinical signs and symptoms include feeding difficulties in infancy, various dental anomalies (dental crowding, dental caries, hypodontia, and oligodontia), behavioral issues (ADHD, autism spectrum disorder, anxiety, obsessive-compulsive disorder, frustration intolerance, and aggressive behavior), refractive error, muscular hypotonia, and common facial dysmorphisms. Regarding the function of the immune system, these individuals show impaired T cell development, with low numbers of RTEs, and low frequencies of ILC2s. They commonly suffer from frequent infections (∼50%) and have an increased risk of developing asthma and allergies (∼40%, Tables 1 and S2). In addition, distinct abnormalities of the skull were found in 38% of affected individuals, including craniosynostosis, scaphocephaly, microcephaly, macrocephaly, and dolichocephaly. Moreover, we document the occurrence of short stature, clinodactyly, retrognathia, and hypothyroidism (Table 1). These LGD variants result in either haploinsufficiency or truncated proteins with loss of at least the last two C-terminal DNA-binding zinc-finger domains (C2H2-ZnFs). *In vitro* analyses, using two exemplary frameshift variants, p.Ser817Ala*fs*\*27 and p.Cys833Trp*fs*\*11, have shown that both result in reduced DNA-binding affinity without exerting a dominant-negative effect on the BCL11B targets analyzed in this study.

Individuals harboring a heterozygous *BCL11B* missense variant affecting a zinc-binding residue within C2H2-

ZnFs mostly display clinical similarities to the individuals harboring LGD variants. Individuals 37–39, harboring p.His842Pro, p.His846Asp, or p.His877Tyr, respectively, were affected by GDD with behavioral issues. Two had hyperopia and feeding difficulties in early childhood. Although we were unable to obtain fresh blood samples for immune phenotyping, two were reported to have eosinophilia, asthma, and allergies. Similar clinical presentation, a neurodevelopmental delay with asthma, and a primary atopic disorder were reported in two individuals harboring *de novo* missense variants that affect a zinc-binding cysteine residue within C2H2_ZnF5, p.Cys826Arg and p.Cys826Tyr.[44] Our *in vitro* analyses, using the exemplary variant p.His842Pro, suggested that these missense variants lead to reduced DNA-binding affinity and may additionally exert a dominant-negative effect in a target-dependent manner, therefore confirming the importance of zinc coordination for the proper folding and stability of the C2H2-ZnFs.[2]

The phenotypic variability is even more pronounced in individuals harboring missense variants affecting the DNA-contacting α helix within a C2H2-ZnF that affect neither a zinc-binding residue nor a "specificity residue." We observed interfamilial phenotypic variability in individuals 27–30, all harboring the p.Cys808Arg variant. Twins (individuals 27 and 28) presented with moderate speech and motor developmental delay, poor fine motor skills, hyperkinetic movement disorder, and behavioral

issues, while their father (individual 30) had poor fine motor skills and late-onset, mild hyperkinetic movement disorder. All members of the family had an intact ILC2 compartment, and the changes in the T cell compartment were rather mild, except in individual 28, who had a very high frequency of γδ-T cells. Both individuals (individuals 31 and 32) harboring the *de novo* p.Ser836Asn variant displayed many clinical similarities to the individuals harboring LGD variants. Individual 32, however, developed acute T cell lymphoblastic leukemia, while individual 31, at age 2 years, does not have a malignancy but has a profoundly affected T cell compartment and reduced ILC2s, similar to individuals harboring LGD variants. Following unremarkable early development, individual 35, harboring a *de novo* p.Thr840Met variant, developed mild intellectual disability, developmental coordination disorder, ADHD, and subcortical myoclonias at the age of 4 years. This individual had a minor alteration in the T cell compartment, with slightly high frequency of γδ-T cells. Notably, reduced DNA-binding affinity for p.Cys808Arg was observed only at the *LTBP3* locus and for p.Ser836Asn at *SHANK3* and *LTBP3* loci. Contrarily, p.Thr840Met displayed impaired DNA-binding affinity at all three analyzed loci and seems to exert a dominant-negative effect on *SHANK3* and *LTBP3* loci. These findings suggest that observed phenotypic and immune variability results from the impaired DNA-binding affinity in a locus-specific and dosage-dependent manner.

Finally, the *BCL11B* subtype characterized by the most severe clinical outcome and largest clinical heterogeneity is attributable to the missense variants affecting one of the four "specificity residues" within C2H2-ZnFs. Indeed, such missense variants result in multisystem anomalies with SCID[30] or syndromic ICL leading to early demise due to infections (individuals 23 and 24; p.Lys469Asn) but also in isolated, severe epileptic encephalopathy (individual 25; p.Arg472Cys). In addition, somewhat comparable to the individuals harboring LGD variants, individual 36, harboring a *de novo* p.Arg841Leu variant, had GDD, autistic features, food allergies, and asthma. Immunodeficiency, either SCID or ICL, was observed exclusively in individuals harboring a missense variant affecting the "specificity residue" at amino acid position +3 (p.Asn441Lys, p.Lys469Asn, p.Asn810His, and p.Lys838Thr) (Figure 2 and Table 2). Similarly, brain MRI abnormalities, gait abnormalities, and seizures, rarely observed in individuals harboring an LGD variant, were more common (>50%) in individuals harboring a "specificity residue"-affecting missense variant. Dystonia, involuntary movements, and cerebral palsy were observed in both individuals harboring the p.Lys838Arg variant, which was extremely rare in individuals harboring an LGD variant (3%–6%). These data suggest that such missense variants exert a more severe effect than the LGD variants on the protein function. Interestingly, the reporter assay revealed that whereas all of the analyzed missense variants affecting a "specificity residue" impair DNA-binding affinity in a similar manner, they differ in seemingly target-specific dominant-negative effects. The clinical variability is likely further explained by alterations in DNA-binding specificity as revealed by the modeling approaches (Figures 4 and S3) and already confirmed for p.Asn441Lys.[30] The latter is further supported by the clinical phenotype of individuals harboring a missense variant at residue Lys838. Namely, individual 33, harboring p.Lys838Thr, did not develop signs of dystonia, involuntary movements, and cerebral palsy, which were observed in both individuals harboring p.Lys838Arg. Similarly, in comparison to individual 33, both individuals harboring p.Lys838Arg did not develop SCID.

Taken together, the clinical, genetic, molecular, and modeling data suggest that the phenotypic diversity of *BCL11B*-related disorders is strongly dependent on the impact of diverse *BCL11B* alterations on its DNA-binding affinity and specificity. LGD variants, resulting either in haploinsufficiency or truncated proteins, with loss of at least the last two C-terminal C2H2-ZnFs leading to reduced DNA-binding affinity, cause a mild to moderate neurodevelopmental delay with increased propensity for behavioral and dental anomalies, allergies, and asthma, and reduced type 2 innate lymphoid cells. A similar clinical course is observed in individuals harboring a missense variant affecting zinc-binding residues, cysteines, and histidines within C2H2-ZnFs. Such missense variants result in reduced DNA-binding affinity and may additionally exert a dominant-negative effect in a target-dependent manner. However, missense variants affecting the DNA-contacting α helix within a C2H2-ZnF that affect neither a zinc-binding residue nor a "specificity residue" result in variable clinical outcomes either similar to those of LGD variants or much milder and later in onset. The comparison of clinical data and results obtained by luciferase assay for other *BCL11B* alterations strongly suggest that their clinical outcome mostly depends on their DNA-binding affinity. The largest clinical heterogeneity and most severe clinical outcomes are observed in individuals harboring a missense variant affecting one of the four "specificity residues" within C2H2-ZnFs. Such missense variants result in reduced DNA-binding affinity and exert a dominant-negative effect in a target-dependent manner. In addition, however, missense variants affecting "specificity residues" result in binding to alternative DNA targets, thus resulting in altered expression of various genes that are not governed by WT BCL11B. Currently, it is impossible to predict such genes and how they will be altered due to such missense variants. Therefore, especially in a prenatal setting, it is impossible to predict their clinical outcome.

In addition to the three suggested *BCL11B* subtypes, an individual affected by syndromic GDD with craniosynostosis harboring a *de novo* p.Arg3Ser was recently described.[34] The identified missense variant, located within a conserved amino terminus, leads to impaired interaction with the RBBP4-MTA1 complex. It is conceivable that missense variants affecting further specific functional sites within *BCL11B*, e.g., affecting phosphorylation

sites or protein-interacting motifs, might further expand the clinical spectrum.

A further emerging question regarding individuals harboring a causative *BCL11B* variant remains the potentially increased risk for developing a malignancy. The analysis of murine models with *Bcl11b* alterations[17,25] and the somatic data of hematologic malignancies[26–29] suggest that BCL11B may act both as a tumor suppressor and as an oncogene. We report here two individuals harboring *BCL11B* variants, a frameshift variant and p.Ser836Asn, who developed a hematologic malignancy. However, it is arguable whether an incidence of ~2% (2/92) allows establishment of *BCL11B* as a tumor predisposition gene. The fact that both developed a different type of malignancy, namely T cell large granular lymphocytic leukemia and T cell acute lymphoblastic leukemia, does not currently allow recommendation of meaningful surveillance strategies.

Beyond the interfamilial variability in individuals 27–30, harboring p.Cys808Arg, several identical *de novo* variants result in variable clinical presentation. All three individuals harboring heterozygous p.Gly630Thr*fs*\*91 included in this study developed a skull abnormality. However, they are very different. Individual 9 had scaphocephaly, individual 10 developed secondary microcephaly, and individual 11 had macrocephaly. Moreover, an individual harboring p.Asn441Lys identical to the initially described *BCL11B* variant[30] had a somewhat milder clinical course, especially in terms of immunodeficiency, compared to the initial case.[32] Similarly, despite harboring the identical p.Asn807Lys variant, neither the here described individual 26 nor the previously reported individual[38] developed a congenital erosive dermatitis that we have documented previously.[31] Likewise, despite many similarities between individuals 23 and 24, both harboring *de novo* p.Lys469Asn, only individual 23 developed pigmentary mosaicism of the skin and white hair, which may be explained by the different nucleotide substitution c.1407G>T and c.1407G>C. Obviously, we cannot completely exclude the possibility that some of these individuals harbor additional variants or epigenetic alterations that may have modified the phenotype. It is worth noting, however, that DNA-binding affinity and specificity of transcription factors can additionally be altered due to changes within the DNA-binding regions, even resulting in cell-type-specific binding changes.[63] Such alterations, in particular single nucleotide polymorphisms, are thought to underlie the increased risk for common diseases.[64] It is thus reasonable to hypothesize that at least some of the observed clinical variability between individuals harboring an identical *BCL11B* variant might be due to rare or even common alterations within its target sites. Since BCL11B regulates gene expression in a context-dependent manner,[9,10] several integrated multi-omics approaches, including ChIP-seq, whole-genome sequencing, methylation profiling, and RNA sequencing, preferentially performed in various cell types and cell lineages, are required to further elucidate the molecular mechanisms underlying the *BCL11B* phenotypic spectrum. Clearly, such analyses will require extensive further work and will be the main aim of our future studies.

In summary, by comparing the clinical and genetic data of altogether 92 affected individuals harboring a likely pathogenic or pathogenic *BCL11B* variant, we have expanded the known clinical spectrum. Combination of immune phenotyping, ChIP-seq followed by luciferase assays, and molecular modeling suggest that the broad phenotypic spectrum of *BCL11B*-related disorders is mainly due to the differential impact of the variants on its DNA-binding affinity and specificity. Our data further highlight the possibility that specific *BCL11B* missense variants can result in unpredictable clinical outcomes differentially affecting the immune system along with development and function of the brain, skin, and teeth.

## Consortia

The members of the Undiagnosed Diseases Network are Aaron Quinlan, Adeline Vanderve, Adriana Rebelo, Aimee Allworth, Alan H. Beggs, Alden Huang, Alex Paul, Ali Al-Beshri, Alistair Ward, Allyn McConkie-Rosell, Alyssa A. Tran, Andrea Gropman, Andrew B. Crouse, Andrew Stergachis, Anita Beck, Anna Hurst, Anna Raper, Anne Hing, Arjun Tarakad, Ashley Andrews, Ashley McMinn, Ashok Balasubramanyam, Audrey Stephannie C. Maghiro, Barbara N. Pusey Swerdzewski, Ben Afzali, Ben Solomon, Beth A. Martin, Breanna Mitchell, Brendan C. Lanpher, Brendan H. Lee, Brent L. Fogel, Brett H. Graham, Brian Corner, Bruce Korf, Calum A. MacRae, Camilo Toro, Cara Skraban, Carlos A. Bacino, Carson A. Smith, Cecilia Esteves, Changrui Xiao, Chloe M. Reuter, Christina Lam, Christine M. Eng, Claire Henchcliffe, Colleen E. Wahl, Corrine K. Welt, Cynthia J. Tifft, Dana Kiley, Daniel Doherty, Daniel J. Rader, Daniel Wegner, Danny Miller, Daryl A. Scott, Dave Viskochil, David A. Sweetser, David R. Adams, Dawn Earl, Deborah Barbouth, Deborah Krakow, Deepak A. Rao, Devin Oglesbee, Devon Bonner, Donna Novacic, Dustin Baldridge, Edward Behrens, Edwin K. Silverman, Elaine Seto, Elijah Kravets, Elizabeth A. Burke, Elizabeth Blue, Elizabeth L. Fieg, Elizabeth Rosenthal, Ellen F. Macnamara, Elsa Balton, Emilie D. Douine, Emily Glanton, Emily Shelkowitz, Eric Allenspach, Eric Klee, Eric Vilain, Erin Baldwin, Erin Conboy, Erin E. Baldwin, Erin McRoy, Esteban C. Dell'Angelica, Euan A. Ashley, F. Sessions Cole, Filippo Pinto e Vairo, Frances High, Francesco Vetrini, Francis Rossignol, Fuki M. Hisama, Gabor Marth, Gail P. Jarvik, Gary D. Clark, George Carvalho, Gerard T. Berry, Ghayda Mirzaa, Gill Bejerano, Giorgio Sirugo, Gonench Kilich, Guney Bademci, Heidi Wood, Herman Taylor, Holly K. Tabor, Hongzheng Dai, Hsiao-Tuan Chao, Hugo J. Bellen, Ian Glass, Ian R. Lanza, Ingrid A. Holm, Isaac S. Kohane, Ivan Chinn, J. Carl Pallais, Jacinda B. Sampson, James P. Orengo, Jason Hom, Jennefer N. Kohler, Jennifer E. Posey, Jennifer

Wambach, Jessica Douglas, Jiayu Fu, Jill A. Rosenfeld, Jimann Shin, Jimmy Bennett, Joan M. Stoler, Joanna M. Gonzalez, John A. Phillips III, John Carey, John J. Mulvihill, Joie Davis, Jonathan A. Bernstein, Jordan Whitlock, Jose Abdenur, Joseph Loscalzo, Joy D. Cogan, Julian A. Martínez-Agosto, Justin Alvey, Kahlen Darr, Kaitlin Callaway, Kathleen A. Leppig, Kathleen Sullivan, Kathy Sisco, Kathyrn Singh, Katrina Dipple, Kayla M. Treat, Kelly Hassey, Kelly Schoch, Kevin S. Smith, Khurram Liaqat, Kim Worley, Kimberly Ezell, Kimberly LeBlanc, Kumarie Latchman, Lance H. Rodan, Laura Pace, Laurel A. Cobban, Lauren C. Briere, Leoyklang Petcharet, LéShon Peart, Lili Mantcheva, Lilianna Solnica-Krezel, Lindsay C. Burrage, Lindsay Mulvihill, Lisa Schimmenti, Lisa T. Emrick, Lorenzo Botto, Lorraine Potocki, Lynette Rives, Lynne A. Wolfe, Manish J. Butte, Margaret Delgado, Maria T. Acosta, Marie Morimoto, Mariko Nakano-Okuno, Mark Wener, Marla Sabaii, Martha Horike-Pyne, Martin G. Martin, Martin Rodriguez, Matt Velinder, Matthew Coggins, Matthew Might, Matthew T. Wheeler, Maura Ruzhnikov, MayChristine V. Malicdan, Meghan C. Halley, Melissa Walker, Michael Bamshad, Michael F. Wangler, Miguel Almalvez, Mohamad Mikati, Monika Weisz Hubshman, Monte Westerfield, Mustafa Tekin, Naghmeh Dorrani, Neil H. Parker, Neil Hanchard, Nicholas Borja, Nicola Longo, Nicole M. Walley, Nina Movsesyan, Nitsuh K. Dargie, Oguz Kanca, Orpa Jean-Marie, Page C. Goddard, Paolo Moretti, Patricia A. Ward, Patricia Dickson, Paul G. Fisher, Pengfei Liu, Peter Byers, Pinar Bayrak-Toydemir, Precilla D'Souza, Queenie Tan, Rachel A. Ungar, Rachel Mahoney, Ramakrishnan Rajagopalan, Raquel L. Alvarez, Rebecca C. Spillmann, Rebecca Ganetzky, Rebecca Overbury, Rebekah Barrick, Richard A. Lewis, Richard L. Maas, Rizwan Hamid, Rong Mao, Ronit Marom, Rosario I. Corona, Russell Butterfield, Sam Sheppeard, Sanaz Attaripour, Seema R. Lalani, Serena Neumann, Shamika Ketkar, Shamil R. Sunyaev, Shilpa N. Kobren, Shinya Yamamoto, Shirley Sutton, Shruti Marwaha, Sirisak Chanprasert, Stanley F. Nelson, Stephan Zuchner, Stephanie Bivona, Stephanie M. Ware, Stephen Pak, Steven Boyden, Suman Jayadev, Surendra Dasari, Susan Korrick, Suzanne Sandmeyer, Tahseen Mozaffar, Tammi Skelton, Tara Wenger, Terra R. Coakley, Thomas Cassini, Thomas J. Nicholas, Timothy Schedl, Tiphanie P. Vogel, Vaidehi Jobanputra, Valerie V. Maduro, Vandana Shashi, Virginia Sybert, Vishnu Cuddapah, Wendy Introne, Wendy Raskind, Willa Thorson, William A. Gahl, William E. Byrd, William J. Craigen, Yan Huang, and Yigit Karasozen.

## Author contributions

I.L. and D.L generated and analyzed the functional data. A. Baresic analyzed the ChIP-sequencing data. J.M. and E.T. generated and analyzed the immune phenotype data. N.M. and D.S. performed cell sorting of frameshift variants. I.L., A. Baresic, E.T., and D.L. wrote the manuscript. The remaining authors provided primary biomaterial (analyzed by J.M. and E.T.) and clinical and genetic data (analyzed by I.L. and D.L.). All authors discussed results, commented on the manuscript, and approved the final manuscript.

## Declaration of interests

Baylor College of Medicine (BCM) and Miraca Holdings Inc. have formed a joint venture with shared ownership and governance of the Baylor Genetics (BG), which performs clinical exome sequencing. J.R.L. has stock ownership in 23andMe, is a paid consultant for Genome International, and is a co-inventor on multiple United States and European patents related to molecular diagnostics for inherited neuropathies, eye diseases, genomic disorders, and bacterial genomic fingerprinting. A. Begtrup is an employee of and may hold stock in GeneDx, LLC.

## Data and code availability

This article includes all datasets generated or analyzed during this study. The raw next-generation sequencing data that support the findings in affected individuals cannot be made publicly available for reasons of patient confidentiality. Qualified researchers may apply for access to these data, pending institutional review board approval (contact D.L., davor.lessel@klinik.uni-regensburg.de).

## Supplemental information

Supplemental information can be found online at https://doi.org/10.1016/j.ajhg.2024.12.012.

## References

1. Vaquerizas, J.M., Kummerfeld, S.K., Teichmann, S.A., and Luscombe, N.M. (2009). A census of human transcription factors: function, expression and evolution. Nat. Rev. Genet. *10*, 252–263. https://doi.org/10.1038/nrg2538.

2. Wolfe, S.A., Nekludova, L., and Pabo, C.O. (2000). DNA recognition by Cys2His2 zinc finger proteins. Annu. Rev. Biophys. Biomol. Struct. *29*, 183–212. https://doi.org/10.1146/annurev.biophys.29.1.183.

3. Persikov, A.V., Wetzel, J.L., Rowland, E.F., Oakes, B.L., Xu, D.J., Singh, M., and Noyes, M.B. (2015). A systematic survey of the Cys2His2 zinc finger DNA-binding landscape. Nucleic Acids Res. *43*, 1965–1984. https://doi.org/10.1093/nar/gku1395.

4. Najafabadi, H.S., Mnaimneh, S., Schmitges, F.W., Garton, M., Lam, K.N., Yang, A., Albu, M., Weirauch, M.T., Radovani, E., Kim, P.M., et al. (2015). C2H2 zinc finger proteins greatly expand the human regulatory lexicon. Nat. Biotechnol. *33*, 555–562. https://doi.org/10.1038/nbt.3128.

5. Cassandri, M., Smirnov, A., Novelli, F., Pitolli, C., Agostini, M., Malewicz, M., Melino, G., and Raschellà, G. (2017). Zinc-finger proteins in health and disease. Cell Death Discov. *3*, 17071. https://doi.org/10.1038/cddiscovery.2017.71.

6. Sommer, R.J., Retzlaff, M., Goerlich, K., Sander, K., and Tautz, D. (1992). Evolutionary conservation pattern of zinc-finger domains of Drosophila segmentation genes. Proc. Natl. Acad. Sci. USA *89*, 10782–10786. https://doi.org/10.1073/pnas.89.22.10782.

7. Al-Naama, N., Mackeh, R., and Kino, T. (2020). C2H2-Type Zinc Finger Proteins in Brain Development, Neurodevelopmental, and Other Neuropsychiatric Disorders: Systematic Literature-Based Analysis. Front. Neurol. *11*, 32. https://doi.org/10.3389/fneur.2020.00032.

8. Lennon, M.J., Jones, S.P., Lovelace, M.D., Guillemin, G.J., and Brew, B.J. (2017). Bcl11b-A Critical Neurodevelopmental Transcription Factor-Roles in Health and Disease. Front. Cell. Neurosci. *11*, 89. https://doi.org/10.3389/fncel.2017.00089.

9. Hosokawa, H., Romero-Wolf, M., Yang, Q., Motomura, Y., Levanon, D., Groner, Y., Moro, K., Tanaka, T., and Rothenberg, E.V. (2020). Cell type-specific actions of Bcl11b in early T-lineage and group 2 innate lymphoid cells. J. Exp. Med. *217*, e20190972. https://doi.org/10.1084/jem.20190972.

10. Sidwell, T., and Rothenberg, E.V. (2021). Epigenetic Dynamics in the Function of T-Lineage Regulatory Factor Bcl11b. Front. Immunol. *12*, 669498. https://doi.org/10.3389/fimmu.2021.669498.

11. Arlotta, P., Molyneaux, B.J., Jabaudon, D., Yoshida, Y., and Macklis, J.D. (2008). Ctip2 controls the differentiation of medium spiny neurons and the establishment of the cellular architecture of the striatum. J. Neurosci. *28*, 622–632. https://doi.org/10.1523/JNEUROSCI.2986-07.2008.

12. Simon, R., Wiegreffe, C., and Britsch, S. (2020). Bcl11 Transcription Factors Regulate Cortical Development and Function. Front. Mol. Neurosci. *13*, 51. https://doi.org/10.3389/fnmol.2020.00051.

13. Golonzhka, O., Metzger, D., Bornert, J.M., Bay, B.K., Gross, M.K., Kioussi, C., and Leid, M. (2009). Ctip2/Bcl11b controls ameloblast formation during mammalian odontogenesis. Proc. Natl. Acad. Sci. USA *106*, 4278–4283. https://doi.org/10.1073/pnas.0900568106.

14. Golonzhka, O., Liang, X., Messaddeq, N., Bornert, J.M., Campbell, A.L., Metzger, D., Chambon, P., Ganguli-Indra, G., Leid, M., and Indra, A.K. (2009). Dual role of COUP-TF-interacting protein 2 in epidermal homeostasis and permeability barrier formation. J. Invest. Dermatol. *129*, 1459–1470. https://doi.org/10.1038/jid.2008.392.

15. Kyrylkova, K., Iwaniec, U.T., Philbrick, K.A., and Leid, M. (2016). BCL11B regulates sutural patency in the mouse craniofacial skeleton. Dev. Biol. *415*, 251–260. https://doi.org/10.1016/j.ydbio.2015.10.010.

16. Inoue, J., Ihara, Y., Tsukamoto, D., Yasumoto, K., Hashidume, T., Kamimura, K., Nakai, Y., Hirano, S., Shimizu, M., Kominami, R., and Sato, R. (2016). Identification of BCL11B as a regulator of adipogenesis. Sci. Rep. *6*, 32750. https://doi.org/10.1038/srep32750.

17. Wakabayashi, Y., Watanabe, H., Inoue, J., Takeda, N., Sakata, J., Mishima, Y., Hitomi, J., Yamamoto, T., Utsuyama, M., Niwa, O., et al. (2003). Bcl11b is required for differentiation and survival of alphabeta T lymphocytes. Nat. Immunol. *4*, 533–539. https://doi.org/10.1038/ni927.

18. Li, P., Burke, S., Wang, J., Chen, X., Ortiz, M., Lee, S.C., Lu, D., Campos, L., Goulding, D., Ng, B.L., et al. (2010). Reprogramming of T cells to natural killer-like cells upon Bcl11b deletion. Science *329*, 85–89. https://doi.org/10.1126/science.1188063.

19. Li, L., Leid, M., and Rothenberg, E.V. (2010). An early T cell lineage commitment checkpoint dependent on the transcription factor Bcl11b. Science *329*, 89–93. https://doi.org/10.1126/science.1188989.

20. Ikawa, T., Hirose, S., Masuda, K., Kakugawa, K., Satoh, R., Shibano-Satoh, A., Kominami, R., Katsura, Y., and Kawamoto, H. (2010). An essential developmental checkpoint for production of the T cell lineage. Science *329*, 93–96. https://doi.org/10.1126/science.1188995.

21. Walker, J.A., Oliphant, C.J., Englezakis, A., Yu, Y., Clare, S., Rodewald, H.R., Belz, G., Liu, P., Fallon, P.G., and McKenzie, A.N.J. (2015). Bcl11b is essential for group 2 innate lymphoid cell development. J. Exp. Med. *212*, 875–882. https://doi.org/10.1084/jem.20142224.

22. Yu, Y., Wang, C., Clare, S., Wang, J., Lee, S.C., Brandt, C., Burke, S., Lu, L., He, D., Jenkins, N.A., et al. (2015). The transcription factor Bcl11b is specifically expressed in group 2 innate lymphoid cells and is essential for their development. J. Exp. Med. *212*, 865–874. https://doi.org/10.1084/jem.20142318.

23. Califano, D., Cho, J.J., Uddin, M.N., Lorentsen, K.J., Yang, Q., Bhandoola, A., Li, H., and Avram, D. (2015). Transcription Factor Bcl11b Controls Identity and Function of Mature Type 2 Innate Lymphoid Cells. Immunity *43*, 354–368. https://doi.org/10.1016/j.immuni.2015.07.005.

24. Wakabayashi, Y., Inoue, J., Takahashi, Y., Matsuki, A., Kosugi-Okano, H., Shinbo, T., Mishima, Y., Niwa, O., and Kominami, R. (2003). Homozygous deletions and point mutations of the Rit1/Bcl11b gene in gamma-ray induced mouse thymic lymphomas. Biochem. Biophys. Res. Commun. *301*, 598–603. https://doi.org/10.1016/s0006-291x(02)03069-3.

25. Go, R., Hirose, S., Morita, S., Yamamoto, T., Katsuragi, Y., Mishima, Y., and Kominami, R. (2010). Bcl11b heterozygosity promotes clonal expansion and differentiation arrest of thymocytes in gamma-irradiated mice. Cancer Sci. *101*, 1347–1353. https://doi.org/10.1111/j.1349-7006.2010.01546.x.

26. Gutierrez, A., Kentsis, A., Sanda, T., Holmfeldt, L., Chen, S.C., Zhang, J., Protopopov, A., Chin, L., Dahlberg, S.E., Neuberg, D.S., et al. (2011). The BCL11B tumor suppressor is mutated across the major molecular subtypes of T-cell acute

lymphoblastic leukemia. Blood *118*, 4169–4173. https://doi.org/10.1182/blood-2010-11-318873.

27. Liu, Y., Easton, J., Shao, Y., Maciaszek, J., Wang, Z., Wilkinson, M.R., McCastlain, K., Edmonson, M., Pounds, S.B., Shi, L., et al. (2017). The genomic landscape of pediatric and young adult T-lineage acute lymphoblastic leukemia. Nat. Genet. *49*, 1211–1218. https://doi.org/10.1038/ng.3909.

28. Di Giacomo, D., La Starza, R., Gorello, P., Pellanera, F., Kalender Atak, Z., De Keersmaecker, K., Pierini, V., Harrison, C.J., Arniani, S., Moretti, M., et al. (2021). 14q32 rearrangements deregulating BCL11B mark a distinct subgroup of T-lymphoid and myeloid immature acute leukemia. Blood *138*, 773–784. https://doi.org/10.1182/blood.2020010510.

29. Montefiori, L.E., Bendig, S., Gu, Z., Chen, X., Pölönen, P., Ma, X., Murison, A., Zeng, A., Garcia-Prat, L., Dickerson, K., et al. (2021). Enhancer Hijacking Drives Oncogenic BCL11B Expression in Lineage-Ambiguous Stem Cell Leukemia. Cancer Discov. *11*, 2846–2867. https://doi.org/10.1158/2159-8290.CD-21-0145.

30. Punwani, D., Zhang, Y., Yu, J., Cowan, M.J., Rana, S., Kwan, A., Adhikari, A.N., Lizama, C.O., Mendelsohn, B.A., Fahl, S.P., et al. (2016). Multisystem Anomalies in Severe Combined Immunodeficiency with Mutant BCL11B. N. Engl. J. Med. *375*, 2165–2176. https://doi.org/10.1056/NEJMoa1509164.

31. Lessel, D., Gehbauer, C., Bramswig, N.C., Schluth-Bolard, C., Venkataramanappa, S., van Gassen, K.L.I., Hempel, M., Haack, T.B., Baresic, A., Genetti, C.A., et al. (2018). BCL11B mutations in patients affected by a neurodevelopmental disorder with reduced type 2 innate lymphoid cells. Brain *141*, 2299–2311. https://doi.org/10.1093/brain/awy173.

32. Alfei, E., Cattaneo, E., Spaccini, L., Iascone, M., Veggiotti, P., and Doneda, C. (2022). Progressive Clinical and Neuroradiological Findings in a Child with BCL11B Missense Mutation: Expanding the Phenotypic Spectrum of Related Disorder. Neuropediatrics *53*, 283–286. https://doi.org/10.1055/s-0041-1736193.

33. Che, F., Tie, X., Lei, H., Zhang, X., Duan, M., Zhang, L., and Yang, Y. (2022). Identification of two novel variants of the BCL11B gene in two Chinese pedigrees associated with neurodevelopmental disorders. Front. Mol. Neurosci. *15*, 927357. https://doi.org/10.3389/fnmol.2022.927357.

34. Goos, J.A.C., Vogel, W.K., Mlcochova, H., Millard, C.J., Esfandiari, E., Selman, W.H., Calpena, E., Koelling, N., Carpenter, E.L., Swagemakers, S.M.A., et al. (2019). A de novo substitution in BCL11B leads to loss of interaction with transcriptional complexes and craniosynostosis. Hum. Mol. Genet. *28*, 2501–2513. https://doi.org/10.1093/hmg/ddz072.

35. Harrer, P., Leppmeier, V., Berger, A., Demund, S., Winkelmann, J., Berweck, S., and Zech, M. (2022). A de novo BCL11B variant case manifesting with dystonic movement disorder regarding the article "BCL11B-related disorder in two canadian children: Expanding the clinical phenotype (Prasad et al., 2020). Eur. J. Med. Genet. *65*, 104635. https://doi.org/10.1016/j.ejmg.2022.104635.

36. Holmes, T.D., Pandey, R.V., Helm, E.Y., Schlums, H., Han, H., Campbell, T.M., Drashansky, T.T., Chiang, S., Wu, C.Y., Tao, C., et al. (2021). The transcription factor Bcl11b promotes both canonical and adaptive NK cell differentiation. Sci. Immunol. *6*, eabc9801. https://doi.org/10.1126/sciimmunol.abc9801.

37. Lu, H.Y., Sertori, R., Contreras, A.V., Hamer, M., Messing, M., Del Bel, K.L., Lopez-Rangel, E., Chan, E.S., Rehmus, W., Milner, J.D., et al. (2021). A Novel Germline Heterozygous BCL11B Variant Causing Severe Atopic Disease and Immune Dysregulation. Front. Immunol. *12*, 788278. https://doi.org/10.3389/fimmu.2021.788278.

38. Prasad, M., Balci, T.B., Prasad, C., Andrews, J.D., Lee, R., Jurkiewicz, M.T., Napier, M.P., Colaiacovo, S., Guillen Sacoto, M.J., and Karp, N. (2020). BCL11B-related disorder in two canadian children: Expanding the clinical phenotype. Eur. J. Med. Genet. *63*, 104007. https://doi.org/10.1016/j.ejmg.2020.104007.

39. Qiao, F., Wang, C., Luo, C., Wang, Y., Shao, B., Tan, J., Hu, P., and Xu, Z. (2019). A De Novo heterozygous frameshift mutation identified in BCL11B causes neurodevelopmental disorder by whole exome sequencing. Mol. Genet. Genomic Med. *7*, e897. https://doi.org/10.1002/mgg3.897.

40. Yang, S., Kang, Q., Hou, Y., Wang, L., Li, L., Liu, S., Liao, H., Cao, Z., Yang, L., and Xiao, Z. (2020). Mutant BCL11B in a Patient With a Neurodevelopmental Disorder and T-Cell Abnormalities. Front. Pediatr. *8*, 544894. https://doi.org/10.3389/fped.2020.544894.

41. Zhao, X., Wu, B., Chen, H., Zhang, P., Qian, Y., Peng, X., Dong, X., Wang, Y., Li, G., Dong, C., and Wang, H. (2022). Case report: A novel truncating variant of BCL11B associated with rare feature of craniosynostosis and global developmental delay. Front. Pediatr. *10*, 982361. https://doi.org/10.3389/fped.2022.982361.

42. Yan, S., Wei, Y.S., Yang, Q.Y., Yang, L., Zeng, T., Tang, X.M., Zhao, X.D., and An, Y.F. (2020). [A case report of BCL11B mutation induced neurodevelopmental disorder and literature review]. Zhonghua Er Ke Za Zhi *58*, 223–227. https://doi.org/10.3760/cma.j.issn.0578-1310.2020.03.012.

43. Pande, S., Mascarenhas, S., Venkatraman, A., Bhat, V., Narayanan, D.L., Siddiqui, S., Bielas, S., Girisha, K.M., and Shukla, A. (2023). Further validation of craniosynostosis as a part of phenotypic spectrum of BCL11B-related BAFopathy. Am. J. Med. Genet. *191*, 2175–2180. https://doi.org/10.1002/ajmg.a.63330.

44. Sabbagh, Q., Haghshenas, S., Piard, J., Trouvé, C., Amiel, J., Attié-Bitach, T., Balci, T., Barat-Houari, M., Belonis, A., Boute, O., et al. (2024). Clinico-biological refinement of BCL11B-related disorder and identification of an episignature: A series of 20 unreported individuals. Genet. Med. *26*, 101007. https://doi.org/10.1016/j.gim.2023.101007.

45. Roa-Bautista, A., López-Duarte, M., Paz-Gandiaga, N., San Segundo Arribas, D., and Ocejo-Vinyals, J.G. (2022). Deletion in the BCL11B Gene and Intellectual Developmental Disorder with Speech Delay, Dysmorphic Facies, and T-cell Abnormalities - a Case Report. EJIFCC *33*, 325–333.

46. Eto, K., Machida, O., Yanagishita, T., Shimojima Yamamoto, K., Chiba, K., Aihara, Y., Hasegawa, Y., Nagata, M., Ishihara, Y., Miyashita, Y., et al. (2022). Novel BCL11B truncation variant in a patient with developmental delay, distinctive features, and early craniosynostosis. Hum Genome Var *9*. Hum. Genome Var. *9*, 43. https://doi.org/10.1038/s41439-022-00220-x.

47. Yu, Y., Jia, X., Yin, H., Jiang, H., Du, Y., Yang, F., Yang, Z., and Li, H. (2023). A novel variant in BCL11B in an individual with neurodevelopmental delay: A case report. Mol. Genet. Genomic Med. *11*, e2132. https://doi.org/10.1002/mgg3.2132.

48. Lessel, D., Schob, C., Küry, S., Reijnders, M.R.F., Harel, T., Eldomery, M.K., Coban-Akdemir, Z., Denecke, J., Edvardson, S., Colin, E., et al. (2017). De Novo Missense Mutations in DHX30 Impair Global Translation and Cause a

Neurodevelopmental Disorder. Am. J. Hum. Genet. *101*, 716–724. https://doi.org/10.1016/j.ajhg.2017.09.014.

49. Lessel, D., Zeitler, D.M., Reijnders, M.R.F., Kazantsev, A., Hassani Nia, F., Bartholomäus, A., Martens, V., Bruckmann, A., Graus, V., McConkie-Rosell, A., et al. (2020). Germline AGO2 mutations impair RNA interference and human neurological development. Nat. Commun. *11*, 5797. https://doi.org/10.1038/s41467-020-19572-5.

50. Lee, H., Deignan, J.L., Dorrani, N., Strom, S.P., Kantarci, S., Quintero-Rivera, F., Das, K., Toy, T., Harry, B., Yourshaw, M., et al. (2014). Clinical exome sequencing for genetic identification of rare Mendelian disorders. JAMA *312*, 1880–1887. https://doi.org/10.1001/jama.2014.14604.

51. Retterer, K., Juusola, J., Cho, M.T., Vitazka, P., Millan, F., Gibellini, F., Vertino-Bell, A., Smaoui, N., Neidich, J., Monaghan, K.G., et al. (2016). Clinical application of whole-exome sequencing across clinical indications. Genet. Med. *18*, 696–704. https://doi.org/10.1038/gim.2015.148.

52. Deciphering Developmental Disorders Study (2017). Prevalence and architecture of de novo mutations in developmental disorders. Nature *542*, 433–438. https://doi.org/10.1038/nature21062.

53. Sadedin, S.P., Dashnow, H., James, P.A., Bahlo, M., Bauer, D.C., Lonie, A., Lunke, S., Macciocca, I., Ross, J.P., Siemering, K.R., et al. (2015). Cpipe: a shared variant detection pipeline designed for diagnostic settings. Genome Med. *7*, 68. https://doi.org/10.1186/s13073-015-0191-x.

54. Richards, S., Aziz, N., Bale, S., Bick, D., Das, S., Gastier-Foster, J., Grody, W.W., Hegde, M., Lyon, E., Spector, E., et al. (2015). Standards and guidelines for the interpretation of sequence variants: a joint consensus recommendation of the American College of Medical Genetics and Genomics and the Association for Molecular Pathology. Genet. Med. *17*, 405–424. https://doi.org/10.1038/gim.2015.30.

55. Sibbertsen, F., Glau, L., Paul, K., Mir, T.S., Gersting, S.W., Tolosa, E., and Dunay, G.A. (2022). Phenotypic analysis of the pediatric immune response to SARS-CoV-2 by flow cytometry. Cytometry A. *101*, 220–227. https://doi.org/10.1002/cyto.a.24528.

56. Zhang, J., Lee, D., Dhiman, V., Jiang, P., Xu, J., McGillivray, P., Yang, H., Liu, J., Meyerson, W., Clarke, D., et al. (2020). An integrative ENCODE resource for cancer genomics. Nat. Commun. *11*, 3696. https://doi.org/10.1038/s41467-020-14743-w.

57. Yu, G., Wang, L.G., and He, Q.Y. (2015). ChIPseeker: an R/Bioconductor package for ChIP peak annotation, comparison and visualization. Bioinformatics *31*, 2382–2383. https://doi.org/10.1093/bioinformatics/btv145.

58. Lessel, D., Wu, D., Trujillo, C., Ramezani, T., Lessel, I., Alwasiyah, M.K., Saha, B., Hisama, F.M., Rading, K., Goebel, I., et al. (2017). Dysfunction of the MDM2/p53 axis is linked to premature aging. J. Clin. Invest. *127*, 3598–3608. https://doi.org/10.1172/JCI92171.

59. Persikov, A.V., Rowland, E.F., Oakes, B.L., Singh, M., and Noyes, M.B. (2014). Deep sequencing of large library selections allows computational discovery of diverse sets of zinc fingers that bind common targets. Nucleic Acids Res. *42*, 1497–1508. https://doi.org/10.1093/nar/gkt1034.

60. Chen, S., Francioli, L.C., Goodrich, J.K., Collins, R.L., Kanai, M., Wang, Q., Alföldi, J., Watts, N.A., Vittal, C., Gauthier, L.D., et al. (2024). A genomic mutational constraint map using variation in 76,156 human genomes. Nature *625*, 92–100. https://doi.org/10.1038/s41586-023-06045-0.

61. Karczewski, K.J., Francioli, L.C., Tiao, G., Cummings, B.B., Alföldi, J., Wang, Q., Collins, R.L., Laricchia, K.M., Ganna, A., Birnbaum, D.P., et al. (2020). The mutational constraint spectrum quantified from variation in 141,456 humans. Nature *581*, 434–443. https://doi.org/10.1038/s41586-020-2308-7.

62. ENCODE Project Consortium, Moore, J.E., Purcaro, M.J., Pratt, H.E., Epstein, C.B., Shoresh, N., Adrian, J., Kawli, T., Davis, C.A., Dobin, A., et al. (2020). Expanded encyclopaedias of DNA elements in the human and mouse genomes. Nature *583*, 699–710. https://doi.org/10.1038/s41586-020-2493-4.

63. Funk, C.C., Casella, A.M., Jung, S., Richards, M.A., Rodriguez, A., Shannon, P., Donovan-Maiye, R., Heavner, B., Chard, K., Xiao, Y., et al. (2020). Atlas of Transcription Factor Binding Sites from ENCODE DNase Hypersensitivity Data across 27 Tissue Types. Cell Rep. *32*, 108029. https://doi.org/10.1016/j.celrep.2020.108029.

64. ENCODE Project Consortium (2012). An integrated encyclopedia of DNA elements in the human genome. Nature *489*, 57–74. https://doi.org/10.1038/nature11247.